

# Cellular automata in $d$ dimensions and ground states of spin models in $(d + 1)$ dimensions

Konstantinos Sfairopoulos,\* Luke Causer, Jamie F. Mair, and Juan P. Garrahan  
*School of Physics and Astronomy, University of Nottingham, Nottingham, NG7 2RD, UK and  
Centre for the Mathematics and Theoretical Physics of Quantum Non-Equilibrium Systems,  
University of Nottingham, Nottingham, NG7 2RD, UK*

We show how the trajectories of  $d$ -dimensional cellular automata (CA) can be used to determine the ground states of  $(d + 1)$ -dimensional classical spin models, and we characterise their quantum phase transition, when in the presence of a transverse magnetic field. For each of the 256 one-dimensional elementary CA we explicitly construct the simplest local two-dimensional classical spin model associated to the given CA, and we also describe this method for  $d > 1$  through selected examples. We illustrate our general observations with detailed studies of: (i) the  $d = 1$  CA Rule 150 and its  $d = 2$  four-body plaquette spin model, (ii) the  $d = 2$  CA whose associated model is the  $d = 3$  square-pyramid plaquette model, and (iii) two counter-propagating  $d = 1$  Rule 60 CA that correspond to the two-dimensional Baxter-Wu spin model. For the quantum spin models, we show that the connection to CAs implies a sensitivity on the approach to the thermodynamic limit via finite size scaling for their quantum phase transitions.

## I. INTRODUCTION

In this paper we provide a complete classification of the ground states of a set of two-dimensional classical spin models, through the use of the trajectories of associated one-dimensional cellular automata (CA), irrespective of their boundary conditions. Our method for the characterisation of the ground states extends to spins in arbitrary local spin dimensions and, thus, it can be straightforwardly generalised to higher dimensions to connect  $d$ -dimensional CAs to  $(d + 1)$ -dimensional spin systems, and to various plaquette interaction terms.

Our method is based on reverse-engineering the Hamiltonian of the spin model from the knowledge of its ground states; that is, we obtain “parent” Hamiltonians. The relation of ground state to Hamiltonian is surjective, so for each class we focus on describing the simplest Hamiltonian per ground state. In one dimension we restrict ourselves to elementary CA [1, 2], and characterise all 256 ground state spaces and the corresponding 256 spin models. This method generalises naturally to higher dimensional CAs, which we illustrate with selected 2D examples that give rise to three-dimensional spin models. Irrespective of the boundary conditions, overall the most interesting cases are obtained for systems with periodic boundary conditions (PBC) related to smaller ground state degeneracies. However, we also discuss other boundary conditions.

By the addition of a transverse field term, these quantum spin models would exhibit a ground-state quantum phase transition controlled by the strength of the transverse field. We show that the knowledge of the CA that determines the classical ground states provides enough information together with the various numerical simulations that we use for identifying the characteristics of these quantum phase transitions. This behaviour is similar to what occurs in Ref. [3] for the quantum Newman-Moore model [4–9], whose classical limit [10–14] obeys CA Rule 60.

While we study the whole class of 2D models arising from 1D elementary CAs, we focus especially on Rule 150 [1, 2], whose associated quantum model is also known as the quantum Fibonacci model [15, 16] (see also Ref. [17]). To illustrate how the method generalises to higher dimension, we consider the Square Pyramid model (SPyM) [14, 18] and we describe the properties of its quantum phase transition. Finally, we employ our methodology to the classification of ground states and the quantum phase transition for the quantum Baxter-Wu (qBW) model [19] (which relates to two counter-propagating CAs). We give the Nonlinear models in 2D are discussed in Appx. C.

The rest of the paper is organised as follows. In Sec. II we discuss the dynamics of 1D and 2D CA and the properties of their limit cycles. In Sec. III we describe the  $(d + 1)$ -dimensional classical spin models that can be derived from  $d$ -dimensional CA. In Sec. IV we consider the corresponding quantum spin models and their ground state phase transitions. In Sec. V we give our conclusions. Extra results are presented in the Appendices, including the list of classical spin models emerging from all the elementary 1D CA in Appx. A, other spin models related to non-elementary CA in Appx. B, a brief discussion of some quantum models that emerge from nonlinear CA rules in Appx. C, further details of numerical simulations for system sizes with open boundary conditions (OBC) in Appx. D and a collection of the respective low energy spectra for some system sizes for the models studied in Appx. E.

## II. CELLULAR AUTOMATA AND THEIR ATTRACTOR STRUCTURE

### A. 1D Cellular Automata

Cellular automata describe the discrete-time evolution of an array of sites (or *cells*), belonging to a finite field or its generalizations, which are characterised by a dynamical map (or the *update rule*), and, in general, might not be deterministic or Markovian [1, 2]. While our methods can be applied to CA with any neighbourhood and with elements in any finite field, we will focus on deterministic update rules and elementary

\* ksfairopoulos@gmail.com

CA.

For 1D elementary CA, the neighbourhood of each lattice site is composed of itself and its two neighbouring sites. As a result, in a 3-site neighbourhood and for the finite field  $\mathbb{F}_2$ , there are 8 possibilities, which give 256 1D elementary CA in total [1, 2]. For example, rules 54 and 150 have the update rules [20]

$$\begin{aligned} f_{54}(p, q, r) &= p + q + r + pr \pmod{2} \\ f_{150}(p, q, r) &= p + q + r \pmod{2} \end{aligned} \quad (1)$$

where  $\{p, q, r\}$  describe the values of the sites in the neighbourhood of the site being updated, see Fig. 1(a). Rule 150 constitutes an example of a linear CA, while rule 54 is non-linear. Here we focus mostly on linear rules, and we include a more detailed study of nonlinear rules in Appx. C. Example trajectories from one initial seed and for a stable cycle are shown in Figs. 1(b, c), respectively.

The periodic structure of a given configuration for the time evolution under a certain rule involves a sequence of configurations which get repeated after applying the update rule  $C$  times, defining a cycle of period  $C$ . The time evolution of linear CA can be described in an algebraic-theoretic way, so that a brute force calculation for the period detection is not necessary [2, 21–23]. For an overview of this method, see Ref. [3] and references therein. We here present an example of this approach for rule 150. The local update rule for a row of  $L$  sites can be expressed in matrix form as

$$A_{150} = \begin{bmatrix} 1 & 1 & 0 & \dots & 0 & 0 & 1 \\ 1 & 1 & 1 & \dots & 0 & 0 & 0 \\ 0 & 1 & 1 & \dots & 0 & 0 & 0 \\ \vdots & \vdots & \vdots & \ddots & \vdots & \vdots & \vdots \\ 0 & 0 & 0 & \dots & 1 & 1 & 0 \\ 0 & 0 & 0 & \dots & 1 & 1 & 1 \\ 1 & 0 & 0 & \dots & 0 & 1 & 1 \end{bmatrix}. \quad (2)$$

The matrix  $A_{150}$  can be expressed as

$$A_{150} = I + S_l + S_r \quad (3)$$

with  $S_l$  and  $S_r$  the left and right shift map, respectively, and where PBC are assumed [24]. The construction of the “minimal polynomial” follows. The order of the irreducible polynomials in its decomposition will give the cycle lengths for the cellular automaton. We give the detailed structure of the periods of rule 150 in Table I for sizes up to  $L = 40$ .

## B. 2D cellular automata: SPyM-CA

The basic theory of CA was first formalised for 1D CA, but extensions to higher dimensions [25] describe many fascinating systems, with Conway’s Game of Life being a prime example [1]. For 2D CA the sites form in general a rectangular lattice. In most cases a von Neumann or a Moore neighbourhood are used for the update rule of the CA [25]. For a Moore neighbourhood, updating each site involves taking into

L	C	L	C
3	1	22	1, 31, 62
4	1, 2	23	1, 2047
5	1, 3	24	1, 2, 4
6	1	25	1, 3, 1023
7	1, 7	26	1, 21, 42
8	1, 2, 4	27	1, 7, 511
9	1, 7	28	1, 2, 7, 14, 28
10	1, 3, 6	29	1, 16383
11	1, 31	30	1, 3, 5, 6, 10, 15, 30
12	1, 2	31	1, 15, 30
13	1, 21	32	1, 2, 4, 8, 16
14	1, 7, 14	33	1, 31
15	1, 3, 5, 15	34	1, 15, 30
16	1, 2, 4, 8	35	1, 3, 7, 21, 4095
17	1, 15	36	1, 2, 7, 14, 28
18	1, 7, 14	37	1, 29127
19	1, 511	38	1, 511, 1022
20	1, 2, 3, 6, 12	39	1, 21, 4095
21	1, 7, 63	40	1, 3, 4, 6, 12, 24

TABLE I: **Invariant cycles of rule 150.** Distinct periods,  $C$ , of invariant cycles for systems of size  $L$  and PBC. Note that this table lists only the distinct periods (including invariant states of period  $C = 1$ ), but not their multiplicities.

account the  $3 \times 3$  square of nearest and next-nearest neighbours [26], while for a von Neumann neighbourhood only the first.

Out of the vast set of possible 2D CAs, we will focus on one which, as shown below, relates to the 3D square pyramid model (SPyM) of Refs. [14, 18]. The 3D SPyM is a generalisation of the 2D triangular plaquette model (TPM) [10–12] whose associated 1D CA is rule 60,

$$f_{60}(p, q, r) = p + q \pmod{2}. \quad (4)$$

Rule 60 generalises to 2D to the update rule for the “SPyM” CA

$$f_{\text{SPyM}}(p_1, \dots, p_9) = p_5 + p_6 + p_8 + p_9 \pmod{2}, \quad (5)$$

where the sites of the Moore neighbourhood are named by row [27]. From now on, the labelling convention  $(p_5, p_6, p_8, p_9) = (p, q, r, s)$  (see Fig. 2) will be used.

With the rule defined, the next task concerns the classification of the attractor structure of the model. Since the SPyM rule is linear, its time evolution can be described in an algebraic-theoretic way, following Refs. [2, 3, 21–23, 28]. For example, for an initial  $3 \times 3$  array we can express the evolution matrix as

$$A_{\text{SPyM}} = \begin{bmatrix} D & 0 & D \\ D & D & 0 \\ 0 & D & D \end{bmatrix}, \quad (6)$$

with

$$D_{3 \times 3} = \begin{bmatrix} 1 & 0 & 1 \\ 1 & 1 & 0 \\ 0 & 1 & 1 \end{bmatrix}. \quad (7)$$

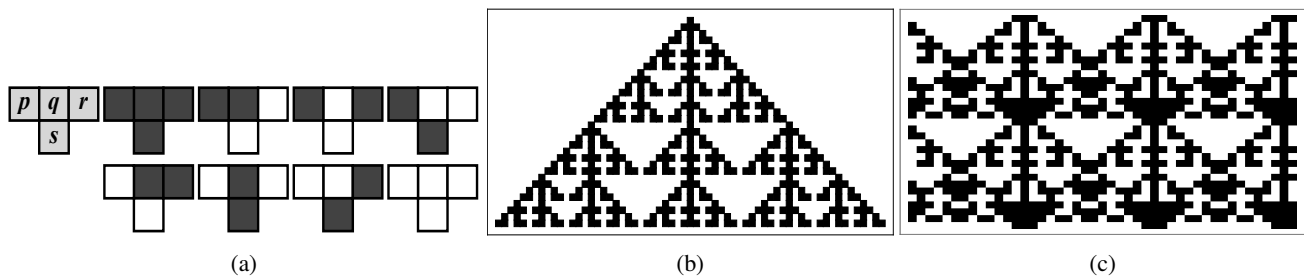


FIG. 1: **CA rule 150.** (a) The local update rule for rule 150.  $\{p, q, r\}$  denote the values of the sites in the neighbourhood of  $q$ , which determine the value of the site  $s$  in the next time step. (b) The evolution from a single initial down site under rule 150. (c) One of the stable cycles of rule 150.

This generalises so that the matrix  $A_{SPyM}$  can be expressed for square systems of odd size as [29]

$$A_{SPyM} = D \otimes D, \quad (8)$$

where  $D$  is the matrix for the evolution of rule 60.

Computing the periods of the stable cycles for the 2D SPyM-CA is a generalisation of the calculation for the rule 60. For example, for lattices where one dimension is a power of two there is a single fixed point (“cycle” of period 1) with all sites up. Table II gives an indicative structure for the periodic behaviour of the SPyM-CA for square initial arrays of size  $L \times L$  (there are many more non-square arrangements which we do not discuss here.) The number of ground states for each period can be also verified through the implementation of Floyd’s “*tortoise and hare*” algorithm.

It is important mentioning that, although SPyM originates to Rule 60, its fixed point structure is different from that of Rule 60; when  $L$  or  $M$  are a power of 2, we still observe a single fixed point, the trivial one. For other system sizes there might exist multiple fixed points, e.g. for a system size  $3 \times 3 \times 4$  there exist 4. The multiplicity of periodic orbits of a given period grows extremely fast. For example, for a  $6 \times 6$  lattice there are 10840 periods of length 6, 80 periods of length 3, 120 periods of length 2, and 16 fixed points.

### III. CLASSICAL SPIN MODELS FROM CA

#### A. Two-dimensional spin models

We first construct the 2D spin models on the square lattice whose ground states are given by 1D CA rules. This method generalises Ref. [3] to all 1D elementary CA. Based on these CA we construct the “simplest” (i.e. most local and lowest order interaction) classical Hamiltonians whose minimum energy configurations are given by the stable cycles of the CA. In Appx. A we list these classical Hamiltonians for the 256 elementary CA.

The 2D spin models we consider live on a square lattice, where the time direction of the CA maps into the second spatial direction of the spin model. The interactions in the spin Hamiltonian are between sites that form the CA neighbourhood, cf. Fig. 1a. This allows for up to four-spin interactions,

L	C
3	1, 3
4	1
5	1, 3, 5, 15
6	1, 2, 3, 6
7	1, 7
8	1
9	1, 3, 7, 21, 63
10	1, 3, 5, 6, 10, 15, 30
11	1, 31, 341
12	1, 3, 4, 6, 12
13	1, 63, 91, 273, 819
14	1, 2, 7, 14
15	1, 3, 5, 15
16	1
17	1, 5, 15, 17, 51, 85, 255
18	1, 2, 3, 6, 7, 14, 21, 42, 63, 126
19	1, 511, 9709
20	1, 3, 5, 12, 15, 20, 30, 60
21	1, 3, 7, 9, 21, 63
22	1, 31, 62, 341, 682
23	1, 89, 2047
24	1, 3, 6, 8, 12, 24
25	1, 3, 5, 15, 775, 1023, 2325, 5115, 8525, 25575
26	1, 63, 91, 126, 182, 273, 546, 819, 1638
27	1, 3, 7, 21, 63, 511, 1533, 1971, 4599, 13797
28	1, 4, 7, 14, 28
29	1, 3683, 16383, 158369, 475107
30	1, 2, 3, 5, 6, 10, 15, 30

TABLE II: **Invariant cycles of the SPyM-CA.** Distinct periods  $\mathcal{C}$  of invariant cycles for systems of size  $L \times L$  and PBC.

including triangular plaquette interactions (if we shear a triangular lattice into a square one). The classification of all the 256 spin models given in Appx. A is obtained from the combination of the eight “fundamental” models with the following

Hamiltonians,

$$E_0 = - \sum_s \sigma_s \quad (9)$$

$$E_{240} = - \sum_{\{p,s\} \in \searrow} \sigma_p \sigma_s \quad (10)$$

$$E_{204} = - \sum_{\{q,s\} \in \downarrow} \sigma_q \sigma_s \quad (11)$$

$$E_{170} = - \sum_{\{r,s\} \in \swarrow} \sigma_r \sigma_s \quad (12)$$

$$E_{60} = - \sum_{\{p,q,s\} \in \nabla} \sigma_p \sigma_q \sigma_s \quad (13)$$

$$E_{90} = - \sum_{\{p,r,s\} \in \nabla} \sigma_p \sigma_r \sigma_s \quad (14)$$

$$E_{102} = - \sum_{\{q,r,s\} \in \nabla} \sigma_q \sigma_r \sigma_s \quad (15)$$

$$E_{150} = - \sum_{\{p,q,r,s\} \in \nabla} \sigma_p \sigma_q \sigma_r \sigma_s, \quad (16)$$

where  $\sigma_a = 1 - 2a = \pm 1$  with  $a = \{p, q, r, s\}$  indicating both the location of the spin degrees of freedom but also the state of the CA site (up/down being 0/1). The subscript in the Hamiltonian above indicates the associated CA rule. We see from the above that rule 0 corresponds to a non-interacting system; rules 240, 204 and 170 to 1D Ising models along diagonal or vertical directions; rules 60 and 102 to the TPM (and its spatial reflection); rule 90 to the three-spin interaction where the the spin with index  $q$  does not participate in the interaction; and rule 150 to a four-spin interacting model, mapping to the product of rule 90 with the spin labelled  $q$ . All the other 2D models related to the elementary CA are obtained via linear combinations of the models Eqs. (9)-(16), see Appx. A.

The minimum energy configurations of the models defined by Eqs. (9)-(16) are found by using the corresponding CA. The exact set of ground states depends on the nature of the boundary conditions of the spin model. For a model in a lattice of size  $L \times M$  we have four possibilities. The first one is PBC in both lattice directions. In this case the ground states are given by the limit cycles of the associated CA of size  $L$  with PBC in space, cf. Table I. Similarly, for spin models with open boundary conditions (OBC) in the horizontal (or  $x$ ) direction, but PBC in the vertical (or  $y$ ) direction, the ground states come from the commensurate limit cycles of the corresponding CA with OBC in space. Similarly, PBC in the space dimension of the CA and OBC in its time direction would imply that all initial configurations are accepted as ground states for the related spin model, as no further criterion needs to be applied. The number of ground states in this case is  $2^L$ . The last possibility is that of a spin model in a lattice with OBC in both  $x$  and  $y$ . In this case the number of classical ground states is  $2^{L+M-1}$  or  $2^{2L+M-2}$  depending on the span of the interaction, due to the freedom in choosing the first row and the first one or two columns of sites of the  $L \times M$  lattice.

Although our focus was on spin models constructed from elementary CA, there is always the possibility of generalising the above results. We give in Appx. B a very brief overview of some classical spin models which extend the notion of el-

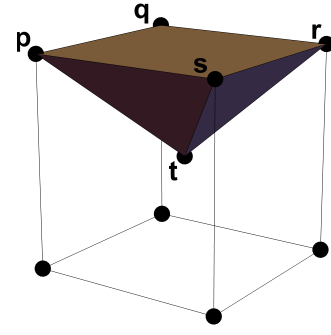


FIG. 2: **Square Pyramid Model.** 5-spin interaction in the SPyM.

ementary CA to larger neighbourhoods or higher dimensions in order to show the versatility of our approach.

### B. 3D spin models: SPyM

For the connection between 2D CA and 3D spin models we focus on the classical model introduced in Ref. [30], termed the square pyramid model (SPyM) in Refs. [14, 18], where it was studied as a model of glasses that generalises the TPM to three dimensions. The classical Hamiltonian of the SPyM is

$$E_{\text{SPyM}} = -J \sum_{\{p,q,r,s,t\} \in \nabla} \sigma_p \sigma_q \sigma_r \sigma_s \sigma_t, \quad (17)$$

where the spins interact on downward pointing pyramids on a BCC lattice, see Fig. 2.

The Hamiltonian (17) is the simplest “parent” Hamiltonian whose classical ground states are determined from the dynamics of the 2D SPyM-CA of Sec. II B. The same considerations relating to boundary conditions as for 2D spin systems apply here. For the SPyM with PBC, the minima are given by the fixed points and commensurate invariant cycles of the SPyM-CA, see Table II. For the SPyM with OBC in a BCC lattice of size  $K \times L \times M$ , the number of ground states is  $2^{K+L+M-2}$ . A similar analysis based on 2D CA can be performed for the ground states of the other 3D spin models of Ref. [30].

### C. Baxter-Wu model and CA rule 60

The Baxter-Wu (BW) model [19, 31–33] is a spin model on the triangular lattice with three-body interactions between both upward and downward pointing triangular plaquettes. Its Hamiltonian reads

$$E_{\text{BW}} = - \sum_{\nabla} \sigma_p \sigma_q \sigma_s - \sum_{\Delta} \sigma_s \sigma_r \sigma_p, \quad (18)$$

where the location of the spins is sketched in Fig. 3 (where again we have represented the triangular lattices sheared into a square lattice). The energy function above is the sum of a TPM (downward pointing plaquettes) and a vertically inverted TPM (upward pointing plaquettes). While the ground states of

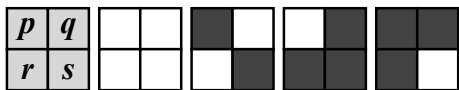


FIG. 3: **Baxter-Wu model.** The labelling for the  $2 \times 2$  blocks, and the accepted combinations, where white/black indicate up/down sites.

the TPM can be inferred from the 1D CA rule 60, the minimum energy configurations of (18) are given by *two counter-propagating* rule 60 CA, see Fig. 3: the forward propagating rule 60 minimizes the first sum in (18), while the backward propagating minimises the second sum. The minimisation of (18) involves the simultaneous minimisation of both CA trajectories, which imposes the restriction

$$p + q = s, \quad s + r = p \pmod{2}, \quad (19)$$

where as before  $\{p, q, r, s\}$  represent the values of the CA sites, see Fig. 3.

Based on the above considerations, the BW model has always the trivial (all spins up) ground state regardless of boundary conditions. For PBC, a BW model of size  $L \times M$  has four ground states if  $L$  and  $M$  are multiples of 3 and only the trivial ground state otherwise. For OBC the BW model always has 4 ground states [34].

#### IV. QUANTUM SPIN MODELS AND GROUND STATE PHASE TRANSITIONS

In this section, we minimally couple the models of section III by adding a transverse field to their Hamiltonians,

$$H_\mu = JE_\mu(Z) - h \sum_{p=1}^N X_p, \quad (20)$$

where we use  $H_\mu$  to denote the quantum Hamiltonian, and  $E_\mu(Z)$  the classical energy function for the spin system related to CA with rule  $\mu$ , cf. Eqs.(9)-(18), with the Ising spin  $\sigma_i$  at site  $i$  replaced by the Pauli operator  $Z_i$ . The balance between classical interactions and transverse field is controlled by the ratio of the coupling strength  $J$  to the field strength  $h$ . As expected, this combination of terms creates competing orders between the classical energy which tends to align the spins in the  $z$ -spin direction of the minimum energy configurations, and the transverse field ones. This competition gives rise to a ground state phase transition in the ground state controlled by the ratio  $J/h$ .

For the models of Eqs.(9)-(18), while the configurations which minimise the classical energy do not directly give the quantum ground states in the presence of a field, they do however determine the symmetries of the quantum models [3], and thus we can use the information from the periodic structure of the related CA to infer the existence or not of spontaneous symmetry breaking (SSB). As we explain below, from a finite size analysis based on the CA, we conjecture that in most of the spin models the quantum phase transition is first order,

with the optional addition of SSB for the system sizes where there are multiple classical ground states. This is the scenario that we found in Ref. [3] for the specific case of the quantum Newman-Moore model through its connection to rule 60. For verifying our claims, we present a wealth of results from numerical simulations obtained using exact diagonalisation (ED) [35] (for systems up to 25 sites), matrix product state (MPS) methods [36–38] (with bond dimensions up to 1000), and continuous-time quantum Monte Carlo (ctQMC) simulations [39–42] (with  $\beta = 100$  or bigger) [43].

#### A. 2D quantum spin models

The quantum spin model (20) with interaction energies related to rules 170, 204 and 240, Eqs. (10)-(12), provides multiple copies of the 1D TFIM embedded in a 2D lattice, while for rule 0 we have a non-interacting spin system with longitudinal and transverse fields. The model connected to rule 60, Eq. (13), is the quantum Newman-Moore model studied in Ref. [3], and rule 102, Eq. (15), is directly related to it by a reflection symmetry. Rule 90 and Eq. (14), although technically distinct from rule 60 when PBC are used, it displays very similar behaviour. We therefore choose to study rule 150, Eq. (16).

The Hamiltonian for the quantum spin model connected to CA rule 150 is

$$H_{150} = -J \sum_{\{p,q,r,s\} \in \nabla} Z_p Z_q Z_r Z_s - h \sum_i X_i. \quad (21)$$

Similar to the case of the quantum Newman-Moore model [4], it is easy to prove (following for example Ref. [44]) that  $H_{150}$  has a duality that exchanges the interaction and field terms in (21). This suggests that, if a quantum phase transition exists, it will be observed on the self-dual point  $J = h$  [45]. The relevant observables to describe the transition are the normalised transverse magnetisation,  $M_x = \frac{1}{N} \sum_i X_i$ , and the longitudinal

magnetisation,  $M_z = \frac{1}{N} \sum_i Z_i$ , and the four-spin interaction operator  $M_{zzzz} = \frac{1}{N} \sum_{\{p,q,r,s\} \in \nabla} Z_p Z_q Z_r Z_s$ .

Figure 4 provides numerical evidence for the quantum phase transition. In all figures we use  $h = 1.0$  without loss of generality. Panel (a) shows the ground state energy per unit length as a function of  $J$ , for square systems  $L \times L$  and PBC from ED and numerical MPS, showing a pronounced change in slope around  $J = 1.0$ . Panels (b) and (c) show the average transverse magnetisation,  $M_x$ , and the average four-spin interaction,  $M_{zzzz}$ , for both square and rectangular systems from numerical MPS and ctQMC simulations. The jump in these observables at  $J = 1.0$  is a clear indication of a first order transition.

Figure 4(d-f) shows the same quantities for quasi-1D geometries, where the first order transition is also present, but weaker. The difference in the appearance of the transition in the thin stripe geometries of Fig 4(d-f) to the square or wider rectangular ones of Fig. 4(a-c) can be qualitatively explained

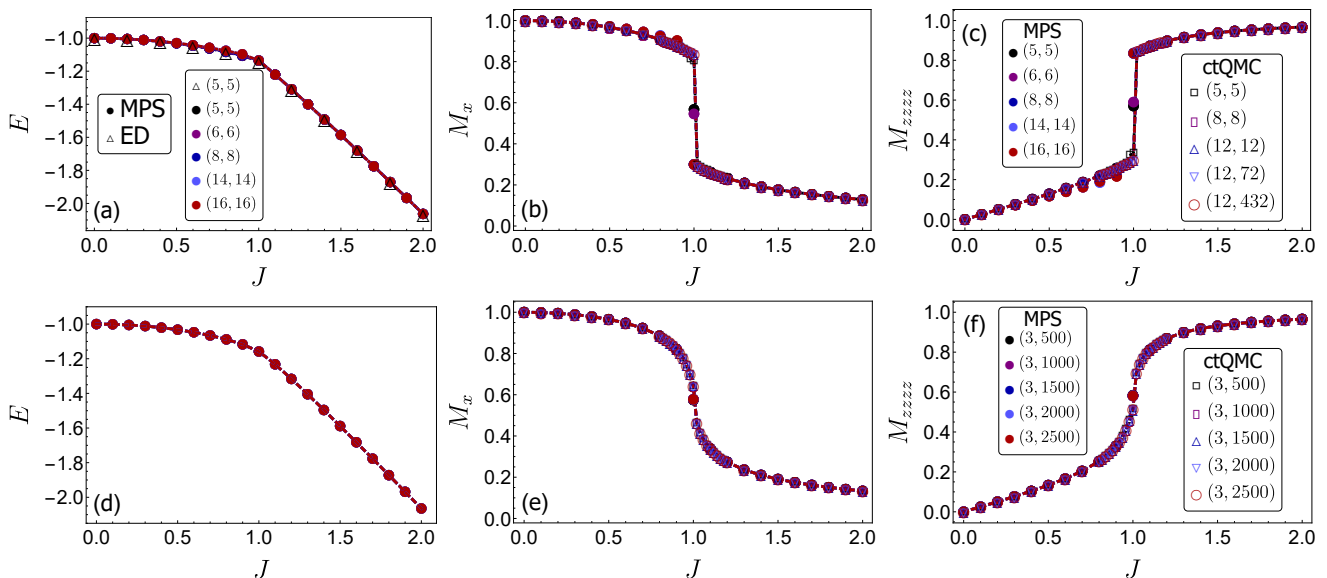


FIG. 4: **Quantum phase transition of  $H_{150}$  for PBC.** (a) The ground state energy  $E$  per unit size as a function of  $J$  for square systems,  $L \times L$ . Empty symbols are from ED while filled symbols are from numerical MPS. (b) The transverse magnetisation  $M_x$  as a function of  $J$ . Here open symbols are from ctQMC simulations, and include wide rectangular systems,  $L \times M$ . (c) Same for the average four-spin interaction  $M_{zzzz}$  (see legends in panel). (d-f) Same but for thin stripe geometries, as indicated in panel (f).

from the behaviour of defects: for very thin stripes excitations are restricted further than in a wider rectangular system size, given the same number of classical ground states; increasing the classical ground states, and therefore the number of low-lying excited states of the quantum model, leads to a reduction of the discontinuity across the first order quantum phase transition. This is similar to what is seen in the quantum Newman-Moore model [3]. The case for OBC is discussed in Appx. D.

The first order quantum phase transition of  $H_{150}$  is related to the nature of the low-lying excitations above the ground state, which in turn are connected to the symmetries of the model. The symmetries of  $H_{150}$  can be obtained as follows: given a system of size  $L \times M$ , for each limit cycle of rule 150 commensurate with those dimensions, cf. Table I, we construct a symmetry operator as the product of  $X$  Pauli matrices acting on the sites where the classical ground state (i.e., the CA cycle) differs from the trivial ground state (all down spins). This is similar to what was done for the quantum TPM,  $H_{60}$ , in Ref. [3], and is an approach applicable to all models for Eq. 9 to Eq. 16. For the case of  $H_{150}$ , given the quartic interactions, there is also the global spin-flip symmetry. While the excitations are difficult to study systematically, there are clear indications of the essential physics from what occurs in small systems. In Appx. E we present the analysis of the low-lying spectrum of the quantum rule 150 and the indication of SSB of the CA symmetries.

We note that only for the cases where Eq. (20) is that of the CA that corresponds to the 1D Ising model, rules 240, 204 and 170, see Eqs. (10)-(12) (or their antiferromagnetic counterparts, rules 15, 51, 85, see Appx. A), we have found the quantum phase transition to be continuous.

## B. 3D models: quantum SPyM

As an example of a 3D quantum spin model we consider the Hamiltonian Eq. (20) with the interaction as in Eq. (17) [46]. The Hamiltonian for this quantum SPyM reads

$$H_{\text{SPyM}} = -J \sum_{\{p,q,r,s,t\} \in \diamond} Z_p Z_q Z_r Z_s Z_t - h \sum_p X_p, \quad (22)$$

where the interactions are described in Fig. 2. The number of classical ground states is given by the cycles of the 2D SPyM-CA, see Table II, which in turn allow to define the symmetries of (22).

The quantum SPyM is a direct generalisation of the quantum Newman-Moore model to 3D. As for the 2D models, it has a duality that exchanges  $J$  and  $h$ , and numerics suggest a quantum phase transition at the self-dual point  $J = h$ , see Fig. 5: for all the sizes studied the numerics for PBC indicate a first order transition at  $J = 1.0$  in the large size limit (where  $h = 1.0$  is assumed). However, in cases where the system allows multiple classical minima from the cycles of the SPyM-CA, the first order transition will be accompanied by SSB. We have verified the numerics of Fig. 5 with ED for systems up to 24 spins. While one would expect MPS approximations to rapidly decrease in accuracy in 3D due to the growth of entanglement, Fig. 2 shows that there is reasonable agreement (for simulations of up to 256 spins) with ctQMC simulations which, in turn, allow one to reach systems of nearly 10000 spins.

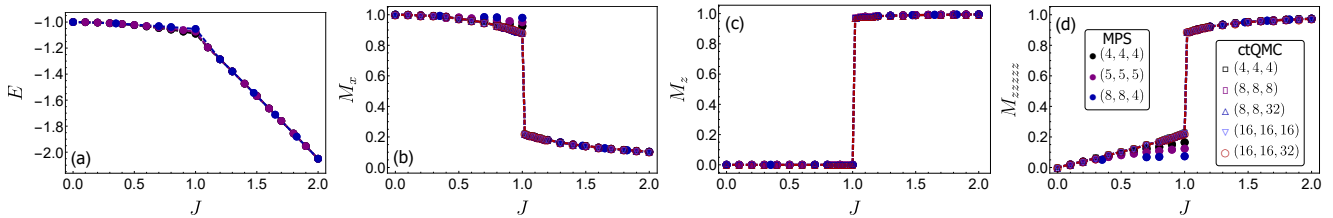


FIG. 5: **Quantum phase transition of  $H_{\text{SPyM}}$  for PBC.** (a) The ground state energy per unit size as a function of  $J$  for system sizes  $L \times L \times M$  (square and rectangular). Filled symbols are from numerical MPS. (b) Transverse magnetisation  $M_x$ . Filled symbols are from numerical MPS and empty symbols from ctQMC. (c,d) Same for longitudinal magnetization  $M_z$ , and average five-spin interaction  $M_{zzzzz}$ , respectively.

### C. The Baxter-Wu model in a transverse field

If in Eq. (20) we use Eq. (18) we obtain the quantum Baxter-Wu model

$$H_{\text{BW}} = -J \sum_{\nabla} Z_p Z_q Z_s - J \sum_{\Delta} Z_s Z_r Z_p - h \sum_p X_p. \quad (23)$$

The Baxter-Wu model in a transverse field was studied in Ref. [19] via stochastic series expansions (SSE) for sizes up to  $15 \times 15$ , finding evidence for a phase transition at  $h \approx 2.4$ .

In Fig. 6 we show our numerics for the quantum Baxter-Wu model. Our results from numerical MPS and ctQMC also suggest a quantum phase transition for at the same position. In panels (a-c) we show square geometries, where our results coincide with those of Ref. [19]. Panels (d-f) show the same for stripe geometries, for which the transition while weaker still seems first order. In the context of our previous analysis, we expect that there will be additional SSB of the classical symmetries for the system sizes that possess multiple classical ground states according to the two counter-propagating CA, cf. Sec. III C.

## V. CONCLUSIONS

In this work we have presented a classification of  $(d+1)$ -dimensional plaquette spin models from the properties of the trajectories of the associated  $d$ -dimensional CA. Given an elementary CA in  $d$  dimensions we have defined the corresponding simplest classical (i.e. that with most local interactions) spin model whose energy is minimised by the trajectories of the CA. For each elementary 1D CA we have provided the associated classical spin model. The set of these 256 models is built from eight fundamental models, each defined by a single kind of interaction, and we focused mostly on the model corresponding to CA Rule 150 which has a four-body interactions. For the case of 2D CA we have considered the rule that gives rise to the SPyM, a 3D generalisation of the TPM.

Endowing these plaquette models with a transverse field, we study their symmetries and we provide evidence for the

existence and for the nature of their ground state phase transitions, based on a range of numerical techniques. We then studied the BW model by the use of two counterpropagating CA. This technique allowed us to uncover the hidden SSB which accompanies its first order quantum phase transition.

Beyond the specific models we considered here, our approach is general and applicable to CA of any neighborhood, in any finite field and in any dimension. Generalizations of the spin models we considered that might be amenable to a similar treatment include those of Ref. [47].

The CA we studied here are all defined in terms of synchronous evolution. A natural generalisation would be to consider CA with dynamics analogous to that of brickwork arrangements as in quantum circuit models [48–56]. Also, we note that some of the models described in Appx. A were also found recently in the context of measurement-induced entanglement phase transitions for random unitary circuits with dissipation [57]. Lastly, the study of these models at finite temperature is another interesting direction: the classical models (in particular those related to nonlinear CA rules) might display glassy dynamics with emergent kinetic constraints, while the finite temperature phase diagram of the respective quantum models might be nontrivial and reveal interesting new phenomena.

## ACKNOWLEDGMENTS

We are grateful to S. Balasubramanian, J.Côté, A. Fahimniya, J. Lahtonen, E.Lake, C. Li, A. Smith, N. Tandivasadakarn, M. Tikhonovskaya and M. Will for various, helpful discussions. We acknowledge financial support from EPSRC Grant no. EP/R04421X/1, the Leverhulme Trust Grant No. RPG-2018-181, and University of Nottingham grant no. FiF1/3. LC was supported by an EPSRC Doctoral prize from the University of Nottingham. Simulations were performed using the University of Nottingham Augusta HPC cluster, and the Sulis Tier 2 HPC platform hosted by the Scientific Computing Research Technology Platform at the University of Warwick (funded by EPSRC Grant EP/T022108/1 and the HPC Midlands+ consortium).

[1] S. Wolfram, Statistical mechanics of cellular automata, *Rev. Mod. Phys.* (1983).

[2] O. Martin, A. M. Odlyzko, and S. Wolfram, Algebraic proper-

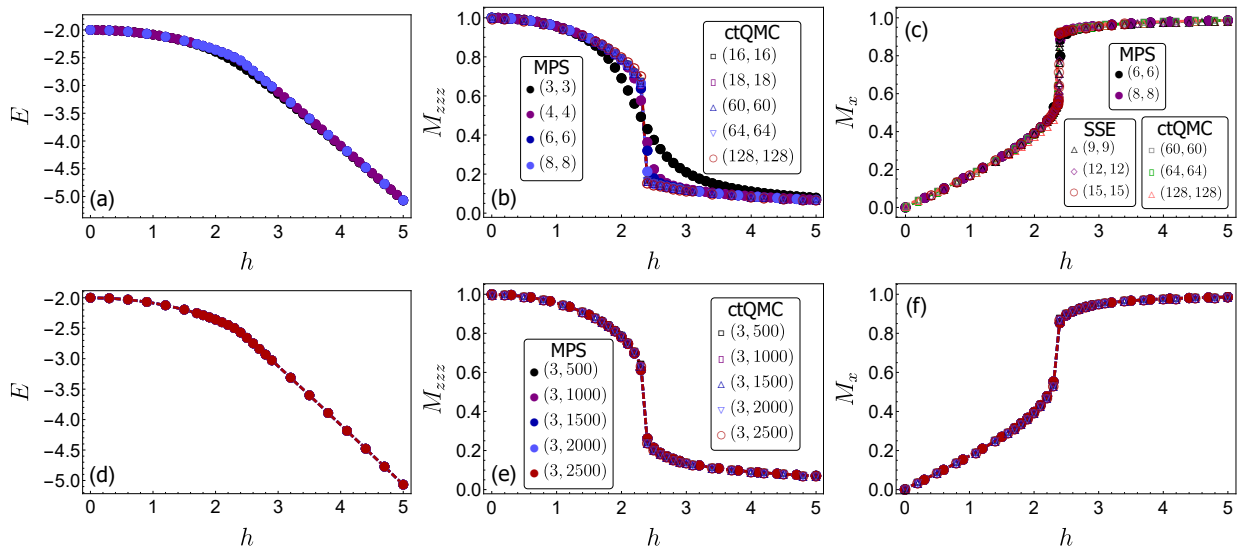


FIG. 6: **Phase transition of  $H_{\text{BW}}$  for PBC.** (a-c) Normalised ground state energy, average three-spin correlator for the interaction from Rule 60 and transverse magnetisation as a function of  $h$  for PBC and square systems sizes, as shown in panel (b). We compare our MPS and ctQMC results to those of Ref. [19] (indicated as SSE) in panel (c) for system sizes as shown in this panel. (d-f) Same but for quasi-1D geometries, as indicated in panel (e).

- ties of cellular automata, *Comm. Math. Phys.* **93**, 219 (1984).
- [3] K. Sfairopoulos, L. Causer, J. F. Mair, and J. P. Garrahan, Boundary conditions dependence of the phase transition in the quantum newman-moore model, [arXiv:2301.02826 \(2023\)](#).
- [4] L. M. Vasiliou, T. H. E. Oakes, F. Carollo, and J. P. Garrahan, Trajectory phase transitions in noninteracting spin systems, *Phys. Rev. E* **101**, 042115 (2020).
- [5] Z. Zhou, X.-F. Zhang, F. Pollmann, and Y. You, Fractal quantum phase transitions: Critical phenomena beyond renormalization, [arXiv:2105.05851 \(2021\)](#).
- [6] E. M. Inack, S. Morawetz, and R. G. Melko, Neural annealing and visualization of autoregressive neural networks in the Newman-Moore model, [arXiv:2204.11272 \(2022\)](#).
- [7] N. Myerson-Jain, K. Su, and C. Xu, Multicritical point with infinite fractal symmetries, *Phys. Rev. B* **106**, 115130 (2022).
- [8] N. E. Myerson-Jain, S. Liu, W. Ji, C. Xu, and S. Vijay, Pascal’s Triangle Fractal Symmetries, *Phys. Rev. Lett.* **128**, 115301 (2022).
- [9] R. Wiedmann, L. Lenke., M. Mühlhauser, and K. P. Schmidt, Absence of fractal quantum criticality in the quantum Newman-Moore model, [arXiv:2302.01773 \(2023\)](#).
- [10] M. E. J. Newman and C. Moore, Glassy dynamics and aging in an exactly solvable spin model, *Phys. Rev. E* **60**, 5068 (1999).
- [11] J. P. Garrahan and M. E. J. Newman, Glassy dynamics of a two-dimensional non-disordered spin model, *AIP Conf. Proc.* **553**, 29 (2001).
- [12] J. P. Garrahan, Glassiness through the emergence of effective dynamical constraints in interacting systems, *J. Phys. Condens. Matt.* **14**, 1571 (2002).
- [13] B. Yoshida, Exotic topological order in fractal spin liquids, *Phys. Rev. B* **88**, 125122 (2013).
- [14] R. M. Turner, R. L. Jack, and J. P. Garrahan, Overlap and activity glass transitions in plaquette spin models with hierarchical dynamics, *Phys. Rev. E* **92** (2015).
- [15] T. Devakul, Y. You, F. J. Burnell, and S. L. Sondhi, Fractal Symmetric Phases of Matter, *SciPost Phys.* **6**, 007 (2019).
- [16] Y. You, T. Devakul, F. J. Burnell, and S. L. Sondhi, Subsystem symmetry protected topological order, *Phys. Rev. B* **98**, 035112 (2018).
- [17] D. T. Stephen, A. Dua, J. Garre-Rubio, D. J. Williamson, and M. Hermele, Fractionalization of subsystem symmetries in two dimensions, *Phys. Rev. B* **106** (2022).
- [18] R. L. Jack and J. P. Garrahan, Phase Transition for Quenched Coupled Replicas in a Plaquette Spin Model of Glasses, *Phys. Rev. Lett.* **116** (2016).
- [19] S. Capponi, S. S. Jahromi, F. Alet, and K. P. Schmidt, Baxter-Wu model in a transverse magnetic field, *Phys. Rev. E* **89**, 062136 (2014).
- [20] The CA we study here are slightly different from those with “Floquet” dynamics which have received much attention recently, such as Rule 54 [49, 58–65], Rule 150 [55, 66, 67] and Rule 201 [52, 68]. The CA we consider have the traditional synchronous dynamics where all sites are updated simultaneously at every time step, while in Floquet-CA one applies successive partial timesteps of commuting transitions in a “brickwork” circuit arrangement.
- [21] E. Jen, Cylindrical cellular automata, *Comm. Math. Phys.* **118**, 569 (1988).
- [22] J. G. Stevens, R. E. Rosensweig, and A. E. Cerkanowicz, Transient and cyclic behavior of cellular automata with null boundary conditions, *J. Stat. Phys.* **73** (1993).
- [23] J. G. Stevens, On the construction of state diagrams for cellular automata with additive rules, *Inf. Sci.* **115**, 43 (1999).
- [24] N. J. Calkin, J. G. Stevens, and D. M. Thomas, A Characterization for the Length of Cycles of the N-Number Ducci Game, *Fibonacci Q.* **43**, 53 (2005).
- [25] N. H. Packard and S. Wolfram, Two-dimensional cellular automata, *J. Stat. Phys.* **38**, 901 (1985).
- [26] S. Wolfram, *A New Kind of Science* (Wolfram Media, 2002).



[27] In the classification of Refs. [1, 2] this 2D CA has rule number  
 5373597862091219546476209478658998037511223013  
 6210049965559464864243992555947294641603678886  
 0722775579758574220861868275515662123592151923  
 6660607363684710

- [28] D. Roy Chowdhury, P. Subbarao, and P. Pal Chaudhuri, Characterization of two-dimensional cellular automata using matrix algebra, *Inf. Sci.* **71**, 289 (1993).
- [29] We thank Jyrki Lahtonen for this observation.
- [30] J. R. Heringa, H. W. J. Blöte, and A. Hoogland, Phase transitions in self-dual Ising models with multispin interactions and a field, *Phys. Rev. Lett.* **63** (1989).
- [31] R. J. Baxter and F. Y. Wu, Exact Solution of an Ising Model with Three-Spin Interactions on a Triangular Lattice, *Phys. Rev. Lett.* **31**, 1294 (1973).
- [32] R. J. Baxter and F. Y. Wu, Ising Model on a Triangular Lattice with Three-spin Interactions. I. The Eigenvalue Equation, *Au. J. Phys.* **27**, 357 (1974).
- [33] R. Baxter, *Exactly Solved Models in Statistical Mechanics*, Dover books on physics (Dover Publications, 2007).
- [34] These arguments can be easily generalised to larger local spin spaces. For example, for spin-1 the number of irreducible-block contributions are 9. These contributions lead to 3 fixed points and, depending on system size, to 2 individual periodic orbits of period 3 (6 states). The irreducible block set,  $S$ , is comprised of the  $2 \times 2$  matrices

$$S = \left\{ \begin{pmatrix} 0 & 0 \\ 0 & 0 \end{pmatrix}, \begin{pmatrix} 2 & 2 \\ 1 & 1 \end{pmatrix}, \begin{pmatrix} 1 & 1 \\ 2 & 2 \end{pmatrix}, \begin{pmatrix} 1 & 0 \\ 0 & 1 \end{pmatrix}, \begin{pmatrix} 2 & 1 \\ 2 & 0 \end{pmatrix}, \right. \\ \left. \begin{pmatrix} 0 & 2 \\ 1 & 2 \end{pmatrix}, \begin{pmatrix} 2 & 0 \\ 0 & 2 \end{pmatrix}, \begin{pmatrix} 0 & 1 \\ 2 & 1 \end{pmatrix}, \begin{pmatrix} 1 & 2 \\ 1 & 0 \end{pmatrix} \right\},$$

where in the first row the 3 blocks giving rise to the 3 fixed points are presented and the contributions of the two periodic orbits occupy the 2nd and 3rd rows, respectively.

- [35] A. W. Sandvik, Computational Studies of Quantum Spin Systems, *AIP Conf. Proc.* **1297**, 135 (2010).
- [36] U. Schollwöck, The density-matrix renormalization group in the age of matrix product states, *Ann. Phys.* **326** (2011).
- [37] E. Stoudenmire and S. R. White, Studying Two-Dimensional Systems with the Density Matrix Renormalization Group, *Annu. Rev. Condens. Matt. Phys.* **3**, 111 (2012).
- [38] M. Fishman, S. R. White, and E. M. Stoudenmire, The ITensor Software Library for Tensor Network Calculations, [arXiv:2007.14822](https://arxiv.org/abs/2007.14822) (2020).
- [39] L. Causser, K. Sfairopoulos, J. F. Mair, and J. P. Garrahan, Rejection-free quantum Monte Carlo in continuous time from transition path sampling, [arXiv:2305.08935](https://arxiv.org/abs/2305.08935) (2023).
- [40] B. B. Beard and U.-J. Wiese, Simulations of Discrete Quantum Systems in Continuous Euclidean Time, *Phys. Rev. Lett.* **77**, 5130 (1996).
- [41] F. Krzakala, A. Rosso, G. Semerjian, and F. Zamponi, Path-integral representation for quantum spin models: Application to the quantum cavity method and Monte Carlo simulations, *Phys. Rev. B* **78**, 134428 (2008).
- [42] T. Mora, A. M. Walczak, and F. Zamponi, Transition path sampling algorithm for discrete many-body systems, *Phys. Rev. E* **85** (2012).
- [43] We note that we can only infer the symmetries of the Hamiltonians corresponding to linear CA rules. The symmetries of the quantum Hamiltonians corresponding to nonlinear rules, cf. Appx. D, do not follow a specific pattern, and the approach described in Sec IV is not applicable. The characterisation of their symmetries in a concise form remains an open issue.
- [44] C. Xu and J. E. Moore, Strong-Weak Coupling Self-Duality in the Two-Dimensional Quantum Phase Transition of  $p + ip$  Superconducting Arrays, *Phys. Rev. Lett.* **93**, 047003 (2004).
- [45] E. Cobanera, G. Ortiz, and Z. Nussinov, The bond-algebraic approach to dualities, *Adv. Phys.* **60**, 679 (2011).
- [46] While the classical SPyM has been considered in the literature, see Refs. [18, 30], to our knowledge, the quantum SPyM has not been studied before.
- [47] S. Biswas, Y. H. Kwan, and S. A. Parameswaran, Beyond the freshman's dream: Classical fractal spin liquids from matrix cellular automata in three-dimensional lattice models, *Phys. Rev. B* **105**, 224410 (2022).
- [48] A. Bobenko, M. Bordemann, C. Gunn, and U. Pinkall, On two integrable cellular automata, *Commun. Math. Phys.* **158**, 127 (1993).
- [49] A. Inoue and S. Takesue, Two extensions of exact nonequilibrium steady states of a boundary-driven cellular automaton, *J. Phys. A: Math. Theor.* **51** (2018).
- [50] B. Bertini, P. Kos, and T. Prosen, Entanglement spreading in a minimal model of maximal many-body quantum chaos, *Phys. Rev. X* **9**, 021033 (2019).
- [51] S. Gopalakrishnan and A. Lamacraft, Unitary circuits of finite depth and infinite width from quantum channels, *Phys. Rev. B* **100**, 064309 (2019).
- [52] J. W. P. Wilkinson, K. Klobas, T. Prosen, and J. P. Garrahan, Exact solution of the Floquet-PXP cellular automaton, *Phys. Rev. E* **102** (2020).
- [53] B. Buča, K. Klobas, and T. Prosen, Rule 54: Exactly solvable model of nonequilibrium statistical mechanics, *J. Stat. Mech.: Theory Exp.* **2021** (7), 074001.
- [54] T. Gombor and B. Pozsgay, Superintegrable cellular automata and dual unitary gates from Yang-Baxter maps, *SciPost Phys.* **12** (2022).
- [55] J. W. P. Wilkinson, T. Prosen, and J. P. Garrahan, Exact solution of the "Rule 150" reversible cellular automaton, *Phys. Rev. E* **105**, 034124 (2022).
- [56] K. Klobas, C. D. Fazio, and J. P. Garrahan, Exact "hydrophobicity" in deterministic circuits: dynamical fluctuations in the Floquet-East model, [arXiv:2305.07423](https://arxiv.org/abs/2305.07423) (2023).
- [57] Y. Li and M. Claassen, Statistical Mechanics of Monitored Dissipative Random Circuits, [arXiv:2303.08152](https://arxiv.org/abs/2303.08152) (2023).
- [58] T. Prosen and C. Mejía-Monasterio, Integrability of a deterministic cellular automaton driven by stochastic boundaries, *J. Phys. A: Math. Theor.* (2016).
- [59] T. Prosen and B. Buča, Exact matrix product decay modes of a boundary driven cellular automaton, *J. Phys. A: Math. Theor.* (2017).
- [60] S. Gopalakrishnan, D. A. Huse, V. Khemani, and R. Vasseur, Hydrodynamics of operator spreading and quasiparticle diffusion in interacting integrable systems, *Phys. Rev. B* **98**, 220303(R) (2018).
- [61] B. Buča, J. P. Garrahan, T. Prosen, and M. Vanicat, Exact large deviation statistics and trajectory phase transition of a deterministic boundary driven cellular automaton, *Phys. Rev. E* **100**, 020103 (2019).
- [62] K. Klobas and T. Prosen, Space-like dynamics in a reversible cellular automaton, *SciPost Phys.* **2**, 010 (2020).
- [63] K. Klobas, M. Medenjak, T. Prosen, and M. Vanicat, Time-dependent matrix product ansatz for interacting reversible dynamics, *Commun. Math. Phys.* **371**, 651 (2019).
- [64] V. Alba, J. Dubail, and M. Medenjak, Operator Entanglement in

Interacting Integrable Quantum Systems: The Case of the Rule 54 Chain, *Phys. Rev. Lett.* **122**, 250603 (2019).

- [65] K. Klobas, M. Vanicat, J. P. Garrahan, and T. Prosen, Matrix product state of multi-time correlations, *J. Phys. A: Math. Theor.* **53**, 335001 (2020).
- [66] S. Gopalakrishnan and B. Zakirov, Facilitated quantum cellular automata as simple models with non-thermal eigenstates and dynamics, *Quantum Sci. Technol.* **3**, 044004 (2018).
- [67] T. Gombor and B. Pozsgay, Integrable spin chains and cellular automata with medium-range interaction, *Phys. Rev. E* **104**, 054123 (2021).
- [68] T. Iadecola and S. Vijay, Nonergodic quantum dynamics from deformations of classical cellular automata, *Phys. Rev. B* **102**, 180302 (2020).
- [69] K. Klobas, B. Bertini, and L. Piroli, Exact Thermalization Dynamics in the “Rule 54” Quantum Cellular Automaton, *Phys. Rev. Lett.* **126**, 160602 (2021).
- [70] K. Klobas and B. Bertini, Entanglement dynamics in Rule 54: Exact results and quasiparticle picture, *SciPost Phys.* **11**, 107 (2021).
- [71] K. Klobas and B. Bertini, Exact relaxation to Gibbs and non-equilibrium steady states in the quantum cellular automaton Rule 54, *SciPost Phys.* **11**, 106 (2021).

### Appendix A: 1D elementary CA and their 2D parent Hamiltonians

Here we present the simplest classical “parent” Hamiltonians for the 256 elementary 1D CA, that is, the energy function

### Appendix B: Other CA and their spin models

Here we discuss how to extend the class of spin models related to CA beyond those presented in the main text. Extending the neighbourhood that defines the CA rule provides us significant freedom to define models with specific properties, e.g. models with specific system sizes that exhibit an exact spin to defect duality, as in Ref. [10]. This feature holds for linear CA which possess an  $A$ -matrix, as in Sec. II A, which is a sum of the diagonal matrix and the left or right shift map (see further details in Ref. [3]). By generalising beyond elementary CA to CA with rules defined on larger neighbourhoods than that of Fig. 1(a), one can obtain other CA with the above property and their corresponding 2D spin models.

Consider a 1D CA with a larger neighbourhood of  $n$  contiguous sites, where we label the sites (and their states)  $(p_1, p_2, \dots, p_n)$  [an elementary CA correspond therefore to  $n = 3$ , and  $(p_1, p_2, p_3) = (p, q, r)$  in Fig. 1(a)]. For example, for  $n = 5$ , three possible rules with this neighbourhood are

$$s = p_1 + p_3, s = p_1 + p_5, s = p_3 + p_5 \pmod{2}, \quad (\text{B1})$$

where  $s$  is the site that gets updated, cf. Fig. 1(a), and the sums are modulo 2. These are related to 2D spin models with a neighbourhood of  $2r + 1$  sites with  $r = 2$  and share the property of a unique minimum energy configuration for certain

with the most local and lowest order interactions for which the cycles of the CA are minimum energy configurations. The relation between a CA rule and the corresponding classical Hamiltonian is given in Tables III-IX. The tables show the CA rule number, the rule for updates in the CA, the local interactions that define the spin model energy function, and the linear combination in terms of the interactions in the irreducible models of Eqs. (9)-(16). Specifically, the energy function for CA rule  $\mu$  is a sum of local interaction terms

$$E_\mu = \sum_{\{p,q,r,s\}} \varepsilon_{p,q,r,s}^{(\mu)}, \quad (\text{A1})$$

where  $\{p, q, r, s\}$  indicate the spins in the neighbourhood like that of Fig. 1. In turn, the interaction  $\varepsilon_{p,q,r,s}^{(\mu)}$  can be written in terms of the interactions of the irreducible models (9)-(16):

$$\varepsilon_{p,q,r,s}^{(\mu)} = \sum_{v \in \text{Irr}} \alpha_v^{(\mu)} \varepsilon_{p,q,r,s}^{(v)} \quad (\text{A2})$$

where “Irr” are the eight irreducible models of Eqs. (9)-(16).

In the table we also use the expressions:

$$J_{a,b} = \frac{1}{2}(1 + \sigma_a + \sigma_b - \sigma_a \sigma_b) \quad (\text{A3})$$

$$K_{a,b,c} = 1 - \frac{1}{4}(1 - \sigma_a - \sigma_b - \sigma_c + \sigma_a \sigma_b + \sigma_a \sigma_c + \sigma_b \sigma_c - \sigma_a \sigma_b \sigma_c). \quad (\text{A4})$$

system sizes.

Similar generalisations to the rule 60 in 3D can be obtained for rules 90 and 150. In terms of the classical spin models, for the 3D version of Eq. (14) we get

$$E_{90}^{(3D)} = - \sum_{\{p_i\}} \sigma_{p_1} \sigma_{p_3} \sigma_{p_7} \sigma_{p_9} \sigma_s, \quad (\text{B2})$$

where  $\{p_1, \dots, p_9\}$  span the Moore neighbourhood. In turn, by generalising Eq. (16) we get

$$E_{150}^{(3D)} = - \sum_{\{p_i\}} \left( \prod_{i=1}^9 \sigma_{p_i} \right) \sigma_s, \quad (\text{B3})$$

where the product includes all spins in the Moore neighbourhood for the update of  $\sigma_s$ . Similar generalisations can be constructed for all other models.

### Appendix C: Nonlinear Rules

Here we consider the case of CA with nonlinear rules and their corresponding spin models. Specifically, we focus on the nonlinear CA rules 30, 54 and 201. Rules 54 and 201 are chosen due to the recent interest in classical and quantum circuits

CA rule no.	Update rule	$\mathcal{E}_{p,q,r,s}^{(\mu)}$	$\alpha_0$	$\alpha_{240}$	$\alpha_{204}$	$\alpha_{170}$	$\alpha_{60}$	$\alpha_{90}$	$\alpha_{102}$	$\alpha_{150}$
0	0	$-\sigma_s$	1	0	0	0	0	0	0	0
1	$1 + p + q + pq + r + pr + qr + pqr$	$\sigma_p \sigma_q \sigma_r \sigma_s J_{p,q} J_{p,r} J_{q,r} K_{p,q,r}$	$\frac{3}{4}$	$-\frac{1}{4}$	$-\frac{1}{4}$	$-\frac{1}{4}$	$-\frac{1}{4}$	$-\frac{1}{4}$	$-\frac{1}{4}$	$-\frac{1}{4}$
2	$r + pr + qr + pqr$	$-\sigma_r \sigma_s J_{p,r} J_{q,r} K_{p,q,r}$	$\frac{3}{4}$	$-\frac{1}{4}$	$-\frac{1}{4}$	$\frac{1}{4}$	$-\frac{1}{4}$	$\frac{1}{4}$	$\frac{1}{4}$	$\frac{1}{4}$
3	$1 + p + q + pq$	$\sigma_p \sigma_q \sigma_s J_{p,q}$	$\frac{1}{2}$	$-\frac{1}{2}$	$-\frac{1}{2}$	0	$-\frac{1}{2}$	0	0	0
4	$q + pq + qr + pqr$	$-\sigma_q \sigma_s J_{p,q} J_{q,r} K_{p,q,r}$	$\frac{3}{4}$	$-\frac{1}{4}$	$\frac{1}{4}$	$-\frac{1}{4}$	$\frac{1}{4}$	$-\frac{1}{4}$	$\frac{1}{4}$	$\frac{1}{4}$
5	$1 + p + r + pr$	$\sigma_p \sigma_r \sigma_s J_{p,r}$	$\frac{1}{2}$	$-\frac{1}{2}$	0	$-\frac{1}{2}$	0	$-\frac{1}{2}$	0	0
6	$q + pq + r + pr$	$-\sigma_q \sigma_r \sigma_s J_{p,q} J_{p,r}$	$\frac{1}{2}$	$-\frac{1}{2}$	0	0	0	0	$\frac{1}{2}$	$\frac{1}{2}$
7	$1 + p + qr + pqr$	$\sigma_p \sigma_s J_{q,r} K_{p,q,r}$	$\frac{1}{4}$	$-\frac{3}{4}$	$-\frac{1}{4}$	$-\frac{1}{4}$	$-\frac{1}{4}$	$-\frac{1}{4}$	$\frac{1}{4}$	$\frac{1}{4}$
8	$qr + pqr$	$-\sigma_s J_{q,r} K_{p,q,r}$	$\frac{1}{4}$	$-\frac{1}{4}$	$\frac{1}{4}$	$\frac{1}{4}$	$\frac{1}{4}$	$\frac{1}{4}$	$-\frac{1}{4}$	$-\frac{1}{4}$
9	$1 + p + q + pq + r + pr$	$\sigma_p \sigma_q \sigma_r \sigma_s J_{p,q} J_{p,r}$	$\frac{1}{2}$	$-\frac{1}{2}$	0	0	0	0	$-\frac{1}{2}$	$-\frac{1}{2}$
10	$r + pr$	$-\sigma_r \sigma_s J_{p,r}$	$\frac{1}{2}$	$-\frac{1}{2}$	0	$\frac{1}{2}$	0	$\frac{1}{2}$	0	0
11	$1 + p + q + pq + qr + pqr$	$\sigma_p \sigma_q \sigma_s J_{p,q} J_{q,r} K_{p,q,r}$	$\frac{1}{4}$	$-\frac{3}{4}$	$-\frac{1}{4}$	$\frac{1}{4}$	$-\frac{1}{4}$	$\frac{1}{4}$	$-\frac{1}{4}$	$-\frac{1}{4}$
12	$q + pq$	$-\sigma_q \sigma_s J_{p,q}$	$\frac{1}{2}$	$-\frac{1}{2}$	$\frac{1}{2}$	0	$\frac{1}{2}$	0	0	0
13	$1 + p + r + pr + qr + pqr$	$\sigma_p \sigma_r \sigma_s J_{p,r} J_{q,r} K_{p,q,r}$	$\frac{1}{4}$	$-\frac{3}{4}$	$\frac{1}{4}$	$-\frac{1}{4}$	$\frac{1}{4}$	$-\frac{1}{4}$	$-\frac{1}{4}$	$-\frac{1}{4}$
14	$q + pq + r + pr + qr + pqr$	$-\sigma_q \sigma_r \sigma_s J_{p,q} J_{p,r} J_{q,r} K_{p,q,r}$	$\frac{1}{4}$	$-\frac{1}{4}$	$\frac{1}{4}$	$\frac{1}{4}$	$\frac{1}{4}$	$\frac{1}{4}$	$\frac{1}{4}$	$\frac{1}{4}$
15	$1 + p$	$\sigma_p \sigma_s$	0	-1	0	0	0	0	0	0
16	$p + pq + pr + pqr$	$-\sigma_p \sigma_s J_{p,q} J_{p,r} K_{p,q,r}$	$\frac{3}{4}$	$\frac{1}{4}$	$-\frac{1}{4}$	$-\frac{1}{4}$	$\frac{1}{4}$	$\frac{1}{4}$	$-\frac{1}{4}$	$\frac{1}{4}$
17	$1 + q + r + qr$	$\sigma_q \sigma_r \sigma_s J_{q,r}$	$\frac{1}{2}$	0	$-\frac{1}{2}$	$-\frac{1}{2}$	0	0	$-\frac{1}{2}$	0
18	$p + pq + r + qr$	$-\sigma_p \sigma_r \sigma_s J_{p,q} J_{q,r}$	$\frac{1}{2}$	0	$-\frac{1}{2}$	0	0	$\frac{1}{2}$	0	$\frac{1}{2}$
19	$1 + q + pr + pqr$	$\sigma_q \sigma_s J_{p,r} K_{p,q,r}$	$\frac{1}{4}$	$-\frac{1}{4}$	$-\frac{3}{4}$	$-\frac{1}{4}$	$-\frac{1}{4}$	$-\frac{1}{4}$	$-\frac{1}{4}$	$-\frac{1}{4}$
20	$p + q + pr + qr$	$-\sigma_p \sigma_q \sigma_s J_{p,r} J_{q,r}$	$\frac{1}{2}$	0	0	$-\frac{1}{2}$	$\frac{1}{2}$	0	0	$\frac{1}{2}$
21	$1 + pq + r + pqr$	$\sigma_r \sigma_s J_{p,q} K_{p,q,r}$	$\frac{1}{4}$	$-\frac{1}{4}$	$-\frac{1}{4}$	$\frac{1}{4}$	$-\frac{1}{4}$	$-\frac{1}{4}$	$-\frac{1}{4}$	$-\frac{1}{4}$
22	$p + q + r + pqr$	$-\sigma_p \sigma_q \sigma_r \sigma_s K_{p,q,r}$	$\frac{1}{4}$	$-\frac{1}{4}$	$-\frac{1}{4}$	$-\frac{1}{4}$	$\frac{1}{4}$	$\frac{1}{4}$	$\frac{1}{4}$	$\frac{3}{4}$
23	$1 + pq + pr + qr$	$\sigma_s J_{p,q} J_{p,r} J_{q,r}$	0	$-\frac{1}{2}$	$-\frac{1}{2}$	$-\frac{1}{2}$	0	0	0	$\frac{1}{2}$
24	$p + pq + pr + qr$	$-\sigma_p \sigma_s J_{p,q} J_{p,r} J_{q,r}$	$\frac{1}{2}$	0	0	0	$\frac{1}{2}$	$\frac{1}{2}$	$-\frac{1}{2}$	0
25	$1 + q + r + pqr$	$\sigma_q \sigma_r \sigma_s K_{p,q,r}$	$\frac{1}{4}$	$-\frac{1}{4}$	$-\frac{1}{4}$	$-\frac{1}{4}$	$\frac{1}{4}$	$\frac{3}{4}$	$-\frac{1}{4}$	$-\frac{1}{4}$
26	$p + pq + r + pqr$	$-\sigma_p \sigma_r \sigma_s J_{p,q} K_{p,q,r}$	$\frac{1}{4}$	$-\frac{1}{4}$	$-\frac{1}{4}$	$\frac{1}{4}$	$\frac{1}{4}$	$\frac{1}{4}$	$-\frac{1}{4}$	$\frac{1}{4}$
27	$1 + q + pr + qr$	$\sigma_q \sigma_s J_{p,r} J_{q,r}$	0	$-\frac{1}{2}$	$-\frac{1}{2}$	0	0	$\frac{1}{2}$	$-\frac{1}{2}$	0
28	$p + q + pr + pqr$	$-\sigma_p \sigma_q \sigma_s J_{p,r} K_{p,q,r}$	$\frac{1}{4}$	$-\frac{1}{4}$	$\frac{1}{4}$	$-\frac{1}{4}$	$\frac{3}{4}$	$\frac{1}{4}$	$-\frac{1}{4}$	$\frac{1}{4}$
29	$1 + pq + r + qr$	$\sigma_r \sigma_s J_{p,q} J_{q,r}$	0	$-\frac{1}{2}$	0	$-\frac{1}{2}$	0	$-\frac{1}{2}$	$-\frac{1}{2}$	0
30	$p + q + r + qr$	$-\sigma_p \sigma_q \sigma_r \sigma_s J_{q,r}$	0	$-\frac{1}{2}$	0	0	$\frac{1}{2}$	$\frac{1}{2}$	0	$\frac{1}{2}$
31	$1 + pq + pr + pqr$	$\sigma_s J_{p,q} J_{p,r} K_{p,q,r}$	$-\frac{1}{4}$	$-\frac{3}{4}$	$-\frac{1}{4}$	$-\frac{1}{4}$	$\frac{1}{4}$	$\frac{1}{4}$	$-\frac{1}{4}$	$-\frac{1}{4}$
32	$pr + pqr$	$-\sigma_s J_{p,r} K_{p,q,r}$	$\frac{3}{4}$	$\frac{1}{4}$	$-\frac{1}{4}$	$\frac{1}{4}$	$-\frac{1}{4}$	$-\frac{1}{4}$	$-\frac{1}{4}$	$-\frac{1}{4}$
33	$1 + p + q + pq + r + qr$	$\sigma_p \sigma_q \sigma_r \sigma_s J_{p,q} J_{q,r}$	$\frac{1}{2}$	0	$-\frac{1}{2}$	0	0	$-\frac{1}{2}$	0	$-\frac{1}{2}$
34	$r + qr$	$-\sigma_r \sigma_s J_{q,r}$	$\frac{1}{2}$	0	$-\frac{1}{2}$	$\frac{1}{2}$	0	0	$\frac{1}{2}$	0
35	$1 + p + q + pq + pr + pqr$	$\sigma_p \sigma_q \sigma_s J_{p,q} J_{p,r} K_{p,q,r}$	$\frac{1}{4}$	$-\frac{1}{4}$	$-\frac{3}{4}$	$\frac{1}{4}$	$-\frac{1}{4}$	$-\frac{1}{4}$	$-\frac{1}{4}$	$-\frac{1}{4}$
36	$q + pq + pr + qr$	$-\sigma_q \sigma_s J_{p,q} J_{p,r} J_{q,r}$	$\frac{1}{2}$	0	0	0	$\frac{1}{2}$	$-\frac{1}{2}$	$\frac{1}{2}$	0
37	$1 + p + r + pqr$	$\sigma_p \sigma_r \sigma_s K_{p,q,r}$	$\frac{1}{4}$	$-\frac{1}{4}$	$-\frac{1}{4}$	$-\frac{1}{4}$	$\frac{1}{4}$	$-\frac{3}{4}$	$\frac{1}{4}$	$-\frac{1}{4}$
38	$q + pq + r + pqr$	$-\sigma_q \sigma_r \sigma_s J_{p,q} K_{p,q,r}$	$\frac{1}{4}$	$-\frac{1}{4}$	$-\frac{1}{4}$	$\frac{1}{4}$	$\frac{1}{4}$	$-\frac{1}{4}$	$\frac{3}{4}$	$\frac{1}{4}$
39	$1 + p + pr + qr$	$\sigma_p \sigma_s J_{p,r} J_{q,r}$	0	$-\frac{1}{2}$	$-\frac{1}{2}$	0	0	$-\frac{1}{2}$	$\frac{1}{2}$	0

TABLE III: 2D classical spin models from 1D CA rules 0 to 39.

built out of these CA (in a Floquet rather than synchronous update arrangement), see e.g. Refs. [52, 56, 64, 69–71].

The update rules for these nonlinear CA are given in Appx. A together with the energies of their corresponding classical spin models. The CA evolution for a single nonzero site is shown in Fig. 7 for the three models. The calculation of the limit cycles for the nonlinear rules cannot be performed in an algebraic-theoretic way as for the linear ones, and one has to resort to brute-force enumeration. For this reason, we employ Floyd’s “*tortoise and hare*” algorithm. Another feature of the nonlinearity concerns the lack of predictive power on the cycle lengths. For additive CA and some specific system

sizes, there exist techniques for the prediction of their cycle lengths. Here, we do not expect any of those techniques to apply.

In Fig. 8 we sketch the attractor structure for these nonlinear rules for some indicative system sizes, in Table X we give the cycle periods for rule 30 up to size  $L = 25$ , and in Table XI for rule 54 up to  $L = 35$ . For rule 201 we always find a periodic structure of an increasing number of fixed points and periods of length 2. The number of these periods (or fixed points) increases sub-extensively, but it is also always bounded by the number of periodic orbits of the OBC case.

The minimal classical spin models whose ground states are

CA rule no.	Update rule	$\mathcal{E}_{p,q,r,s}^{(\mu)}$	$\alpha_0$	$\alpha_{240}$	$\alpha_{204}$	$\alpha_{170}$	$\alpha_{60}$	$\alpha_{90}$	$\alpha_{102}$	$\alpha_{150}$
40	$pr + qr$	$-\sigma_s J_{p,r} J_{q,r}$	$\frac{1}{2}$	0	0	$\frac{1}{2}$	$\frac{1}{2}$	0	0	$-\frac{1}{2}$
41	$1 + p + q + pq + r + pqr$	$\sigma_p \sigma_q \sigma_r \sigma_s J_{p,q} K_{p,q,r}$	$\frac{1}{4}$	$-\frac{1}{4}$	$-\frac{1}{4}$	$\frac{1}{4}$	$\frac{1}{4}$	$-\frac{1}{4}$	$-\frac{1}{4}$	$-\frac{3}{4}$
42	$r + pqr$	$-\sigma_r \sigma_s K_{p,q,r}$	$\frac{1}{4}$	$-\frac{1}{4}$	$-\frac{1}{4}$	$\frac{1}{4}$	$\frac{1}{4}$	$\frac{1}{4}$	$\frac{1}{4}$	$-\frac{1}{4}$
43	$1 + p + q + pq + pr + qr$	$\sigma_p \sigma_q \sigma_s J_{p,q} J_{p,r} J_{q,r}$	0	$-\frac{1}{2}$	$-\frac{1}{2}$	$\frac{1}{2}$	0	0	0	$-\frac{1}{2}$
44	$q + pq + pr + pqr$	$-\sigma_q \sigma_s J_{p,q} J_{p,r} K_{p,q,r}$	$\frac{1}{4}$	$-\frac{1}{4}$	$\frac{1}{4}$	$\frac{1}{4}$	$\frac{3}{4}$	$-\frac{1}{4}$	$\frac{1}{4}$	$-\frac{1}{4}$
45	$1 + p + r + qr$	$\sigma_p \sigma_r \sigma_s J_{q,r}$	0	$-\frac{1}{2}$	0	0	$\frac{1}{2}$	$-\frac{1}{2}$	0	$-\frac{1}{2}$
46	$q + pq + r + qr$	$-\sigma_q \sigma_r \sigma_s J_{p,q} J_{q,r}$	0	$-\frac{1}{2}$	0	$\frac{1}{2}$	$\frac{1}{2}$	0	$\frac{1}{2}$	0
47	$1 + p + pr + pqr$	$\sigma_p \sigma_s J_{p,r} K_{p,q,r}$	$-\frac{1}{4}$	$-\frac{1}{4}$	$-\frac{1}{4}$	$\frac{1}{4}$	$\frac{1}{4}$	$-\frac{1}{4}$	$\frac{1}{4}$	$-\frac{1}{4}$
48	$p + pq$	$-\sigma_p \sigma_s J_{p,q}$	$\frac{1}{2}$	$\frac{1}{2}$	$-\frac{1}{2}$	0	0	0	0	0
49	$1 + q + r + pr + qr + pqr$	$\sigma_q \sigma_r \sigma_s J_{p,r} J_{q,r} K_{p,q,r}$	$\frac{1}{4}$	$\frac{1}{4}$	$-\frac{3}{4}$	$-\frac{1}{4}$	$\frac{1}{4}$	$-\frac{1}{4}$	$-\frac{1}{4}$	$-\frac{1}{4}$
50	$p + pq + r + pr + qr + pqr$	$-\sigma_p \sigma_r \sigma_s J_{p,q} J_{p,r} J_{q,r} K_{p,q,r}$	$\frac{1}{4}$	$\frac{1}{4}$	$-\frac{3}{4}$	$\frac{1}{4}$	$\frac{1}{4}$	$\frac{1}{4}$	$\frac{1}{4}$	$-\frac{1}{4}$
51	$1 + q$	$\sigma_q \sigma_s$	0	0	-1	0	0	0	0	0
52	$p + q + qr + pqr$	$-\sigma_p \sigma_q \sigma_s J_{q,r} K_{p,q,r}$	$\frac{1}{4}$	$\frac{1}{4}$	$-\frac{1}{4}$	$-\frac{1}{4}$	$\frac{3}{4}$	$-\frac{1}{4}$	$\frac{1}{4}$	$\frac{1}{4}$
53	$1 + pq + r + pr$	$\sigma_r \sigma_s J_{p,q} J_{p,r}$	0	0	$-\frac{1}{2}$	$-\frac{1}{2}$	$\frac{1}{2}$	$-\frac{1}{2}$	0	0
54	$p + q + r + pr$	$-\sigma_p \sigma_q \sigma_r \sigma_s J_{p,r}$	0	0	$-\frac{1}{2}$	0	$\frac{1}{2}$	0	$\frac{1}{2}$	$\frac{1}{2}$
55	$1 + pq + qr + pqr$	$\sigma_s J_{p,q} J_{q,r} K_{p,q,r}$	$-\frac{1}{4}$	$-\frac{1}{4}$	$-\frac{3}{4}$	$-\frac{1}{4}$	$\frac{1}{4}$	$-\frac{1}{4}$	$\frac{1}{4}$	$\frac{1}{4}$
56	$p + pq + qr + pqr$	$-\sigma_p \sigma_s J_{p,q} J_{q,r} K_{p,q,r}$	$\frac{1}{4}$	$\frac{1}{4}$	$-\frac{1}{4}$	$\frac{1}{4}$	$\frac{3}{4}$	$\frac{1}{4}$	$-\frac{1}{4}$	$-\frac{1}{4}$
57	$1 + q + r + pr$	$\sigma_q \sigma_r \sigma_s J_{p,r}$	0	0	$-\frac{1}{2}$	0	$\frac{1}{2}$	0	$-\frac{1}{2}$	$-\frac{1}{2}$
58	$p + pq + r + pr$	$-\sigma_p \sigma_r \sigma_s J_{p,q} J_{p,r}$	0	0	$-\frac{1}{2}$	$\frac{1}{2}$	$\frac{1}{2}$	$\frac{1}{2}$	0	0
59	$1 + q + qr + pqr$	$\sigma_q \sigma_s J_{q,r} K_{p,q,r}$	$-\frac{1}{4}$	$-\frac{1}{4}$	$-\frac{3}{4}$	$\frac{1}{4}$	$\frac{1}{4}$	$\frac{1}{4}$	$-\frac{1}{4}$	$-\frac{1}{4}$
60	$p + q$	$-\sigma_p \sigma_q \sigma_s$	0	0	0	0	1	0	0	0
61	$1 + pq + r + pr + qr + pqr$	$\sigma_r \sigma_s J_{p,q} J_{p,r} J_{q,r} K_{p,q,r}$	$-\frac{1}{4}$	$-\frac{1}{4}$	$-\frac{1}{4}$	$-\frac{1}{4}$	$\frac{3}{4}$	$-\frac{1}{4}$	$-\frac{1}{4}$	$-\frac{1}{4}$
62	$p + q + r + pr + qr + pqr$	$-\sigma_p \sigma_q \sigma_r \sigma_s J_{p,r} J_{q,r} K_{p,q,r}$	$-\frac{1}{4}$	$-\frac{1}{4}$	$-\frac{1}{4}$	$\frac{1}{4}$	$\frac{3}{4}$	$\frac{1}{4}$	$\frac{1}{4}$	$\frac{1}{4}$
63	$1 + pq$	$\sigma_s J_{p,q}$	$-\frac{1}{2}$	$-\frac{1}{2}$	$-\frac{1}{2}$	0	$\frac{1}{2}$	0	0	0
64	$pq + pqr$	$-\sigma_s J_{p,q} K_{p,q,r}$	$\frac{3}{4}$	$\frac{1}{4}$	$\frac{1}{4}$	$-\frac{1}{4}$	$-\frac{1}{4}$	$\frac{1}{4}$	$\frac{1}{4}$	$-\frac{1}{4}$
65	$1 + p + q + r + pr + qr$	$\sigma_p \sigma_q \sigma_r \sigma_s J_{p,r} J_{q,r}$	$\frac{1}{2}$	0	0	$-\frac{1}{2}$	0	0	0	$-\frac{1}{2}$
66	$pq + r + pr + qr$	$-\sigma_r \sigma_s J_{p,q} J_{p,r} J_{q,r}$	$\frac{1}{2}$	0	0	0	$-\frac{1}{2}$	$\frac{1}{2}$	$\frac{1}{2}$	0
67	$1 + p + q + pqr$	$\sigma_p \sigma_q \sigma_s K_{p,q,r}$	$\frac{1}{4}$	$-\frac{1}{4}$	$-\frac{1}{4}$	$-\frac{1}{4}$	$-\frac{3}{4}$	$\frac{1}{4}$	$\frac{1}{4}$	$-\frac{1}{4}$
68	$q + qr$	$-\sigma_q \sigma_s J_{q,r}$	$\frac{1}{2}$	0	$\frac{1}{2}$	$-\frac{1}{2}$	0	0	$\frac{1}{2}$	0
69	$1 + p + pq + r + pr + pqr$	$\sigma_p \sigma_r \sigma_s J_{p,q} J_{p,r} K_{p,q,r}$	$\frac{1}{4}$	$-\frac{1}{4}$	$\frac{1}{4}$	$-\frac{3}{4}$	$-\frac{1}{4}$	$-\frac{1}{4}$	$\frac{1}{4}$	$-\frac{1}{4}$
70	$q + r + pr + pqr$	$-\sigma_q \sigma_r \sigma_s J_{p,r} K_{p,q,r}$	$\frac{1}{4}$	$-\frac{1}{4}$	$\frac{1}{4}$	$-\frac{1}{4}$	$-\frac{1}{4}$	$\frac{1}{4}$	$\frac{3}{4}$	$\frac{1}{4}$
71	$1 + p + pq + qr$	$\sigma_p \sigma_s J_{p,q} J_{q,r}$	0	$-\frac{1}{2}$	0	$-\frac{1}{2}$	$-\frac{1}{2}$	0	$\frac{1}{2}$	0
72	$pq + qr$	$-\sigma_s J_{p,q} J_{q,r}$	$\frac{1}{2}$	0	$\frac{1}{2}$	0	0	$\frac{1}{2}$	0	$-\frac{1}{2}$
73	$1 + p + q + r + pr + pqr$	$\sigma_p \sigma_q \sigma_r \sigma_s J_{p,r} K_{p,q,r}$	$\frac{1}{4}$	$-\frac{1}{4}$	$\frac{1}{4}$	$-\frac{1}{4}$	$-\frac{1}{4}$	$\frac{1}{4}$	$-\frac{1}{4}$	$-\frac{3}{4}$
74	$pq + r + pr + pqr$	$-\sigma_r \sigma_s J_{p,q} J_{p,r} K_{p,q,r}$	$\frac{1}{4}$	$-\frac{1}{4}$	$\frac{1}{4}$	$\frac{1}{4}$	$-\frac{1}{4}$	$\frac{3}{4}$	$\frac{1}{4}$	$-\frac{1}{4}$
75	$1 + p + q + qr$	$\sigma_p \sigma_q \sigma_s J_{q,r}$	0	$-\frac{1}{2}$	0	0	$-\frac{1}{2}$	$\frac{1}{2}$	0	$-\frac{1}{2}$
76	$q + pqr$	$-\sigma_q \sigma_s K_{p,q,r}$	$\frac{1}{4}$	$-\frac{1}{4}$	$\frac{3}{4}$	$-\frac{1}{4}$	$\frac{1}{4}$	$\frac{1}{4}$	$\frac{1}{4}$	$-\frac{1}{4}$
77	$1 + p + pq + r + pr + qr$	$\sigma_p \sigma_r \sigma_s J_{p,q} J_{p,r} J_{q,r}$	0	$-\frac{1}{2}$	$\frac{1}{2}$	$-\frac{1}{2}$	0	0	0	$-\frac{1}{2}$
78	$q + r + pr + qr$	$-\sigma_q \sigma_r \sigma_s J_{p,r} J_{q,r}$	0	$-\frac{1}{2}$	$\frac{1}{2}$	0	0	$\frac{1}{2}$	$\frac{1}{2}$	0
79	$1 + p + pq + pqr$	$\sigma_p \sigma_s J_{p,q} K_{p,q,r}$	$-\frac{1}{4}$	$-\frac{3}{4}$	$\frac{1}{4}$	$-\frac{1}{4}$	$-\frac{1}{4}$	$\frac{1}{4}$	$\frac{1}{4}$	$-\frac{1}{4}$

TABLE IV: 2D classical spin models from 1D CA rules 40 to 79.

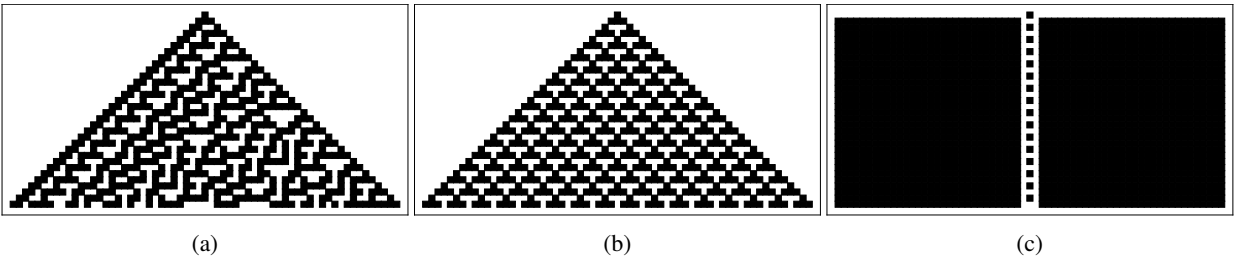


FIG. 7: CA with nonlinear rules. Evolution from a single up site for rules (a) 30, (b) 54 and (c) 201.

CA rule no.	Update rule	$\mathcal{E}_{p,q,r,s}^{(\mu)}$	$\alpha_0$	$\alpha_{240}$	$\alpha_{204}$	$\alpha_{170}$	$\alpha_{60}$	$\alpha_{90}$	$\alpha_{102}$	$\alpha_{150}$
80	$p + pr$	$-\sigma_p \sigma_s J_{p,r}$	$\frac{1}{2}$	$\frac{1}{2}$	0	$-\frac{1}{2}$	0	$\frac{1}{2}$	0	0
81	$1 + q + pq + r + qr + pqr$	$\sigma_q \sigma_r \sigma_s J_{p,q} J_{q,r} K_{p,q,r}$	$\frac{1}{4}$	$\frac{1}{4}$	$-\frac{1}{4}$	$-\frac{3}{4}$	$-\frac{1}{4}$	$\frac{1}{4}$	$-\frac{1}{4}$	$-\frac{1}{4}$
82	$p + r + qr + pqr$	$-\sigma_p \sigma_r \sigma_s J_{q,r} K_{p,q,r}$	$\frac{1}{4}$	$\frac{1}{4}$	$-\frac{1}{4}$	$-\frac{1}{4}$	$-\frac{1}{4}$	$\frac{1}{4}$	$\frac{1}{4}$	$\frac{1}{4}$
83	$1 + q + pq + pr$	$\sigma_q \sigma_s J_{p,q} J_{p,r}$	0	0	$-\frac{1}{2}$	$-\frac{1}{2}$	$-\frac{1}{2}$	$\frac{1}{2}$	0	0
84	$p + q + pq + pr + qr + pqr$	$-\sigma_p \sigma_q \sigma_s J_{p,q} J_{p,r} J_{q,r} K_{p,q,r}$	$\frac{1}{4}$	$\frac{1}{4}$	$\frac{1}{4}$	$-\frac{3}{4}$	$\frac{1}{4}$	$\frac{1}{4}$	$\frac{1}{4}$	$\frac{1}{4}$
85	$1 + r$	$\sigma_r \sigma_s$	0	0	0	-1	0	0	0	0
86	$p + q + pq + r$	$-\sigma_p \sigma_q \sigma_r \sigma_s J_{p,q}$	0	0	0	$-\frac{1}{2}$	0	$\frac{1}{2}$	$\frac{1}{2}$	$\frac{1}{2}$
87	$1 + pr + qr + pqr$	$\sigma_s J_{p,r} J_{q,r} K_{p,q,r}$	$-\frac{1}{4}$	$-\frac{1}{4}$	$-\frac{1}{4}$	$-\frac{3}{4}$	$-\frac{1}{4}$	$\frac{1}{4}$	$\frac{1}{4}$	$\frac{1}{4}$
88	$p + pr + qr + pqr$	$-\sigma_p \sigma_s J_{p,r} J_{q,r} K_{p,q,r}$	$\frac{1}{4}$	$\frac{1}{4}$	$\frac{1}{4}$	$-\frac{1}{4}$	$\frac{1}{4}$	$\frac{1}{4}$	$-\frac{1}{4}$	$-\frac{1}{4}$
89	$1 + q + pq + r$	$\sigma_q \sigma_r \sigma_s J_{p,q}$	0	0	0	$-\frac{1}{2}$	0	$\frac{1}{2}$	$-\frac{1}{2}$	$-\frac{1}{2}$
90	$p + r$	$-\sigma_p \sigma_r \sigma_s$	0	0	0	0	0	1	0	0
91	$1 + q + pq + pr + qr + pqr$	$\sigma_q \sigma_s J_{p,q} J_{p,r} J_{q,r} K_{p,q,r}$	$-\frac{1}{4}$	$-\frac{1}{4}$	$-\frac{1}{4}$	$-\frac{1}{4}$	$-\frac{1}{4}$	$\frac{3}{4}$	$-\frac{1}{4}$	$-\frac{1}{4}$
92	$p + q + pq + pr$	$-\sigma_p \sigma_q \sigma_s J_{p,q} J_{p,r}$	0	0	$\frac{1}{2}$	$-\frac{1}{2}$	$\frac{1}{2}$	$\frac{1}{2}$	0	0
93	$1 + r + qr + pqr$	$\sigma_r \sigma_s J_{q,r} K_{p,q,r}$	$-\frac{1}{4}$	$-\frac{1}{4}$	$\frac{1}{4}$	$-\frac{3}{4}$	$\frac{1}{4}$	$\frac{1}{4}$	$-\frac{1}{4}$	$-\frac{1}{4}$
94	$p + q + pq + r + qr + pqr$	$-\sigma_p \sigma_q \sigma_r \sigma_s J_{p,q} J_{q,r} K_{p,q,r}$	$-\frac{1}{4}$	$-\frac{1}{4}$	$\frac{1}{4}$	$-\frac{1}{4}$	$\frac{1}{4}$	$\frac{1}{4}$	$\frac{1}{4}$	$\frac{1}{4}$
95	$1 + pr$	$\sigma_s J_{p,r}$	$-\frac{1}{2}$	$-\frac{1}{2}$	0	-2	0	2	0	0
96	$pq + pr$	$-\sigma_s J_{p,q} J_{p,r}$	$\frac{1}{2}$	$\frac{1}{2}$	0	0	0	0	$\frac{1}{2}$	$-\frac{1}{2}$
97	$1 + p + q + r + qr + pqr$	$\sigma_p \sigma_q \sigma_r \sigma_s J_{q,r} K_{p,q,r}$	$\frac{1}{4}$	$\frac{1}{4}$	$-\frac{1}{4}$	$-\frac{1}{4}$	$-\frac{1}{4}$	$-\frac{1}{4}$	$\frac{1}{4}$	$-\frac{3}{4}$
98	$pq + r + qr + pqr$	$-\sigma_r \sigma_s J_{p,q} J_{q,r} K_{p,q,r}$	$\frac{1}{4}$	$\frac{1}{4}$	$-\frac{1}{4}$	$-\frac{1}{4}$	$-\frac{1}{4}$	$\frac{1}{4}$	$\frac{3}{4}$	$-\frac{1}{4}$
99	$1 + p + q + pr$	$\sigma_p \sigma_q \sigma_s J_{p,r}$	0	0	$-\frac{1}{2}$	0	$-\frac{1}{2}$	0	$\frac{1}{2}$	$-\frac{1}{2}$
100	$q + pr + qr + pqr$	$-\sigma_q \sigma_s J_{p,r} J_{q,r} K_{p,q,r}$	$\frac{1}{4}$	$\frac{1}{4}$	$\frac{1}{4}$	$-\frac{1}{4}$	$\frac{1}{4}$	$-\frac{1}{4}$	$\frac{3}{4}$	$-\frac{1}{4}$
101	$1 + p + pq + r$	$\sigma_p \sigma_r \sigma_s J_{p,q}$	0	0	0	$-\frac{1}{2}$	0	$-\frac{1}{2}$	$\frac{1}{2}$	$-\frac{1}{2}$
102	$q + r$	$-\sigma_q \sigma_r \sigma_s$	0	0	0	0	0	0	1	0
103	$1 + p + pq + pr + qr + pqr$	$\sigma_p \sigma_s J_{p,q} J_{p,r} J_{q,r} K_{p,q,r}$	$-\frac{1}{4}$	$-\frac{1}{4}$	$-\frac{1}{4}$	$-\frac{1}{4}$	$-\frac{1}{4}$	$-\frac{1}{4}$	$\frac{3}{4}$	$-\frac{1}{4}$
104	$pq + pr + qr + pqr$	$-\sigma_s J_{p,q} J_{p,r} J_{q,r} K_{p,q,r}$	$\frac{1}{4}$	$\frac{1}{4}$	$\frac{1}{4}$	$\frac{1}{4}$	$\frac{1}{4}$	$\frac{1}{4}$	$\frac{1}{4}$	$-\frac{3}{4}$
105	$1 + p + q + r$	$\sigma_p \sigma_q \sigma_r \sigma_s$	0	0	0	0	0	0	0	-1
106	$pq + r$	$-\sigma_r \sigma_s J_{p,q}$	0	0	0	$\frac{1}{2}$	0	$\frac{1}{2}$	$\frac{1}{2}$	$-\frac{1}{2}$
107	$1 + p + q + pr + qr + pqr$	$\sigma_p \sigma_q \sigma_s J_{p,r} J_{q,r} K_{p,q,r}$	$-\frac{1}{4}$	$-\frac{1}{4}$	$-\frac{1}{4}$	$\frac{1}{4}$	$-\frac{1}{4}$	$\frac{1}{4}$	$\frac{1}{4}$	$-\frac{3}{4}$
108	$q + pr$	$-\sigma_q \sigma_s J_{p,r}$	0	0	$\frac{1}{2}$	0	$\frac{1}{2}$	0	$\frac{1}{2}$	$-\frac{1}{2}$
109	$1 + p + pq + r + qr + pqr$	$\sigma_p \sigma_r \sigma_s J_{p,q} J_{q,r} K_{p,q,r}$	$-\frac{1}{4}$	$-\frac{1}{4}$	$\frac{1}{4}$	$-\frac{1}{4}$	$\frac{1}{4}$	$-\frac{1}{4}$	$\frac{3}{4}$	$-\frac{1}{4}$
110	$q + r + qr + pqr$	$-\sigma_q \sigma_r \sigma_s J_{q,r} K_{p,q,r}$	$-\frac{1}{4}$	$-\frac{1}{4}$	$\frac{1}{4}$	$\frac{1}{4}$	$\frac{1}{4}$	$\frac{1}{4}$	$\frac{1}{4}$	$-\frac{1}{4}$
111	$1 + p + pq + pr$	$\sigma_p \sigma_s J_{p,q} J_{p,r}$	$-\frac{1}{2}$	$-\frac{1}{2}$	0	0	0	0	$-\frac{1}{2}$	$-\frac{1}{2}$
112	$p + pqr$	$-\sigma_p \sigma_s K_{p,q,r}$	$\frac{1}{4}$	$\frac{3}{4}$	$-\frac{1}{4}$	$-\frac{1}{4}$	$\frac{1}{4}$	$\frac{1}{4}$	$\frac{1}{4}$	$-\frac{1}{4}$
113	$1 + q + pq + r + pr + qr$	$\sigma_q \sigma_r \sigma_s J_{p,q} J_{p,r} J_{q,r}$	0	$\frac{1}{2}$	$-\frac{1}{2}$	$-\frac{1}{2}$	0	0	0	$-\frac{1}{2}$
114	$p + r + pr + qr$	$-\sigma_p \sigma_r \sigma_s J_{p,r} J_{q,r}$	0	$\frac{1}{2}$	$-\frac{1}{2}$	0	0	$\frac{1}{2}$	$\frac{1}{2}$	0
115	$1 + q + pq + pqr$	$\sigma_q \sigma_s J_{p,q} K_{p,q,r}$	$-\frac{1}{4}$	$\frac{1}{4}$	$-\frac{3}{4}$	$-\frac{1}{4}$	$-\frac{1}{4}$	$\frac{1}{4}$	$\frac{1}{4}$	$-\frac{1}{4}$
116	$p + q + pq + qr$	$-\sigma_p \sigma_q \sigma_s J_{p,q} J_{q,r}$	0	$\frac{1}{2}$	0	$-\frac{1}{2}$	$\frac{1}{2}$	0	$\frac{1}{2}$	0
117	$1 + r + pr + pqr$	$\sigma_r \sigma_s J_{p,r} K_{p,q,r}$	$-\frac{1}{4}$	$\frac{1}{4}$	$-\frac{1}{4}$	$-\frac{3}{4}$	$\frac{1}{4}$	$-\frac{1}{4}$	$\frac{1}{4}$	$-\frac{1}{4}$
118	$p + q + pq + r + pr + pqr$	$-\sigma_p \sigma_q \sigma_r \sigma_s J_{p,q} J_{p,r} K_{p,q,r}$	$-\frac{1}{4}$	$\frac{1}{4}$	$-\frac{1}{4}$	$-\frac{1}{4}$	$\frac{1}{4}$	$\frac{1}{4}$	$\frac{3}{4}$	$\frac{1}{4}$
119	$1 + qr$	$\sigma_s J_{q,r}$	$-\frac{1}{2}$	0	$-\frac{1}{2}$	$-\frac{1}{2}$	0	0	$\frac{1}{2}$	0

TABLE V: 2D classical spin models from 1D CA rules 80 to 119.

described by the nonlinear rules 30, 54 and 201 can be found in Appx. A. For example for rule 201 we have, see Table VIII,

$$E_{201} = -\frac{1}{2}(E_{60} + E_{102} + E_{150} - E_{170}). \quad (C1)$$

We study the quantum version of these models by minimally coupling them to a transverse field. Based on the results above, we also expect these models to have a first order quantum phase transition, with additional SSB in the low-lying spectrum when classical ground state degeneracies exist. Indeed, numerical simulations seem to support this scenario, see Figs. 9,10,11.

Our numerics for these models are not as accurate as those in the main text for the models from linear rules. This is most notable for the numerical MPS, probably due to the fact that the extra terms in the Hamiltonians increase the entanglement close to the phase transition point. That the phase transitions seem to occur at  $J \approx h$  is surprising as in this case there are no duality arguments to suggest it (similarly for the quantum Baxter-Wu model the transition is around  $h \approx 2.4J$ ). Nevertheless, while the numerics are suggestive, more extensive studies will be needed for these models, in order to confirm the existence of the transitions in the thermodynamic limit (see in particular Fig. 11 for  $H_{201}$ ).

CA rule no.	Update rule	$\varepsilon_{p,q,r,s}^{(\mu)}$	$\alpha_0$	$\alpha_{240}$	$\alpha_{204}$	$\alpha_{170}$	$\alpha_{60}$	$\alpha_{90}$	$\alpha_{102}$	$\alpha_{150}$
120	$p + qr$	$-\sigma_p \sigma_s q_r$	0	$\frac{1}{2}$	0	0	$\frac{1}{2}$	$\frac{1}{2}$	0	$-\frac{1}{2}$
121	$1 + q + pq + r + pr + pqr$	$\sigma_q \sigma_r \sigma_s J_{p,q} J_{p,r} K_{p,q,r}$	$-\frac{1}{4}$	$\frac{1}{4}$	$-\frac{1}{4}$	$-\frac{1}{4}$	$\frac{1}{4}$	$\frac{1}{4}$	$-\frac{1}{4}$	$-\frac{3}{4}$
122	$p + r + pr + pqr$	$-\sigma_p \sigma_r \sigma_s J_{p,r} K_{p,q,r}$	$-\frac{1}{4}$	$\frac{1}{4}$	$-\frac{1}{4}$	$\frac{1}{4}$	$\frac{1}{4}$	$\frac{1}{4}$	$-\frac{1}{4}$	$-\frac{1}{4}$
123	$1 + q + pq + qr$	$\sigma_q \sigma_s J_{p,q} J_{q,r}$	$-\frac{1}{2}$	0	$-\frac{1}{2}$	0	0	$\frac{1}{2}$	0	$-\frac{1}{2}$
124	$p + q + pq + pqr$	$-\sigma_p \sigma_q \sigma_s J_{p,q} K_{p,q,r}$	$-\frac{1}{4}$	$\frac{1}{4}$	$\frac{1}{4}$	$-\frac{1}{4}$	$\frac{3}{4}$	$\frac{1}{4}$	$\frac{1}{4}$	$-\frac{1}{4}$
125	$1 + r + pr + qr$	$\sigma_r \sigma_s J_{p,r} J_{q,r}$	$-\frac{1}{2}$	0	0	$-\frac{1}{2}$	$\frac{1}{2}$	0	0	$-\frac{1}{2}$
126	$p + q + pq + r + pr + qr$	$-\sigma_p \sigma_q \sigma_r \sigma_s J_{p,q} J_{p,r} J_{q,r}$	$-\frac{1}{2}$	0	0	0	$\frac{1}{2}$	$\frac{1}{2}$	$\frac{1}{2}$	0
127	$1 + pqr$	$\sigma_s K_{p,q,r}$	$-\frac{3}{4}$	$-\frac{1}{4}$	$-\frac{1}{4}$	$-\frac{1}{4}$	$\frac{1}{4}$	$\frac{1}{4}$	$\frac{1}{4}$	$-\frac{1}{4}$
128	$pqr$	$-\sigma_s K_{p,q,r}$	$\frac{3}{4}$	$\frac{1}{4}$	$\frac{1}{4}$	$\frac{1}{4}$	$-\frac{1}{4}$	$-\frac{1}{4}$	$-\frac{1}{4}$	$\frac{1}{4}$
129	$1 + p + q + pq + r + pr + qr$	$\sigma_p \sigma_q \sigma_r \sigma_s J_{p,q} J_{p,r} J_{q,r}$	$\frac{1}{2}$	0	0	0	$-\frac{1}{2}$	$-\frac{1}{2}$	$-\frac{1}{2}$	0
130	$r + pr + qr$	$-\sigma_r \sigma_s J_{p,r} J_{q,r}$	$\frac{1}{2}$	0	0	$\frac{1}{2}$	$-\frac{3}{2}$	0	0	$\frac{1}{2}$
131	$1 + p + q + pq + pqr$	$\sigma_p \sigma_q \sigma_s J_{p,q} K_{p,q,r}$	$\frac{1}{4}$	$-\frac{1}{4}$	$-\frac{1}{4}$	$\frac{1}{4}$	$-\frac{1}{4}$	$-\frac{1}{4}$	$-\frac{1}{4}$	$\frac{1}{4}$
132	$q + pq + qr$	$-\sigma_q \sigma_s J_{p,q} J_{q,r}$	$\frac{1}{2}$	0	$\frac{1}{2}$	0	0	$-\frac{1}{2}$	0	$\frac{1}{2}$
133	$1 + p + r + pr + pqr$	$\sigma_p \sigma_r \sigma_s J_{p,r} K_{p,q,r}$	$\frac{1}{4}$	$-\frac{1}{4}$	$\frac{1}{4}$	$-\frac{1}{4}$	$-\frac{1}{4}$	$-\frac{1}{4}$	$-\frac{1}{4}$	$\frac{1}{4}$
134	$q + pq + r + pr + pqr$	$-\sigma_q \sigma_r \sigma_s J_{p,q} J_{p,r} K_{p,q,r}$	$\frac{1}{4}$	$-\frac{1}{4}$	$\frac{1}{4}$	$\frac{1}{4}$	$-\frac{1}{4}$	$-\frac{1}{4}$	$-\frac{1}{4}$	$\frac{3}{4}$
135	$1 + p + qr$	$\sigma_p \sigma_s J_{q,r}$	0	$-\frac{1}{2}$	0	0	$-\frac{1}{2}$	$-\frac{1}{2}$	0	$\frac{1}{2}$
136	$qr$	$-\sigma_s J_{q,r}$	$\frac{1}{2}$	0	$\frac{1}{2}$	$\frac{1}{2}$	0	0	$-\frac{1}{2}$	0
137	$1 + p + q + pq + r + pr + pqr$	$\sigma_p \sigma_q \sigma_r \sigma_s J_{p,q} J_{p,r} K_{p,q,r}$	$\frac{1}{4}$	$-\frac{1}{4}$	$\frac{1}{4}$	$\frac{1}{4}$	$-\frac{1}{4}$	$-\frac{1}{4}$	$-\frac{1}{4}$	$-\frac{1}{4}$
138	$r + pr + pqr$	$-\sigma_r \sigma_s J_{p,r} K_{p,q,r}$	$\frac{1}{4}$	$-\frac{1}{4}$	$\frac{1}{4}$	$\frac{1}{4}$	$-\frac{1}{4}$	$-\frac{1}{4}$	$-\frac{1}{4}$	$\frac{1}{4}$
139	$1 + p + q + pq + qr$	$\sigma_p \sigma_q \sigma_s J_{p,q} J_{q,r}$	0	$-\frac{1}{2}$	0	0	$-\frac{1}{2}$	0	$-\frac{1}{2}$	0
140	$q + pq + pqr$	$-\sigma_q \sigma_s J_{p,q} K_{p,q,r}$	$\frac{1}{4}$	$-\frac{1}{4}$	$\frac{3}{4}$	$\frac{1}{4}$	$\frac{1}{4}$	$-\frac{1}{4}$	$-\frac{1}{4}$	$\frac{1}{4}$
141	$1 + p + r + pr + qr$	$\sigma_p \sigma_r \sigma_s J_{p,r} J_{q,r}$	0	$-\frac{1}{2}$	$\frac{1}{2}$	0	0	$-\frac{1}{2}$	$-\frac{1}{2}$	0
142	$q + pq + r + pr + qr$	$-\sigma_q \sigma_r \sigma_s J_{p,q} J_{p,r} J_{q,r}$	0	$-\frac{1}{2}$	$\frac{1}{2}$	$\frac{1}{2}$	0	0	0	$\frac{1}{2}$
143	$1 + p + pqr$	$\sigma_p \sigma_s K_{p,q,r}$	$-\frac{1}{4}$	$-\frac{3}{4}$	$\frac{1}{4}$	$\frac{1}{4}$	$-\frac{1}{4}$	$-\frac{1}{4}$	$-\frac{1}{4}$	$\frac{1}{4}$
144	$p + pq + pr$	$-\sigma_p \sigma_s J_{p,q} J_{p,r}$	$\frac{1}{2}$	$\frac{1}{2}$	0	0	0	0	$-\frac{1}{2}$	$\frac{1}{2}$
145	$1 + q + r + qr + pqr$	$\sigma_q \sigma_r \sigma_s J_{q,r} K_{p,q,r}$	$\frac{1}{4}$	$\frac{1}{4}$	$-\frac{1}{4}$	$-\frac{1}{4}$	$-\frac{1}{4}$	$-\frac{1}{4}$	$-\frac{3}{4}$	$\frac{1}{4}$
146	$p + pq + r + qr + pqr$	$-\sigma_p \sigma_r \sigma_s J_{p,q} J_{q,r} K_{p,q,r}$	$\frac{1}{4}$	$\frac{1}{4}$	$-\frac{1}{4}$	$\frac{1}{4}$	$-\frac{1}{4}$	$\frac{1}{4}$	$-\frac{1}{4}$	$\frac{3}{4}$
147	$1 + q + pr$	$\sigma_q \sigma_s J_{p,r}$	0	0	$-\frac{1}{2}$	0	$-\frac{1}{2}$	0	$-\frac{1}{2}$	$\frac{1}{2}$
148	$p + q + pr + qr + pqr$	$-\sigma_p \sigma_q \sigma_s J_{p,r} J_{q,r} K_{p,q,r}$	$\frac{1}{4}$	$\frac{1}{4}$	$\frac{1}{4}$	$-\frac{1}{4}$	$\frac{1}{4}$	$-\frac{1}{4}$	$-\frac{1}{4}$	$\frac{1}{4}$
149	$1 + pq + r$	$\sigma_r \sigma_s J_{p,q}$	0	0	0	$-\frac{1}{2}$	0	$-\frac{1}{2}$	$-\frac{1}{2}$	$\frac{1}{2}$
150	$p + q + r$	$-\sigma_p \sigma_q \sigma_r \sigma_s$	0	0	0	0	0	0	0	1
151	$1 + pq + pr + qr + pqr$	$\sigma_s J_{p,q} J_{p,r} J_{q,r} K_{p,q,r}$	$-\frac{1}{4}$	$-\frac{1}{4}$	$-\frac{1}{4}$	$-\frac{1}{4}$	$-\frac{1}{4}$	$-\frac{1}{4}$	$-\frac{1}{4}$	$\frac{3}{4}$
152	$p + pq + pr + qr + pqr$	$-\sigma_p \sigma_s J_{p,q} J_{p,r} J_{q,r} K_{p,q,r}$	$\frac{1}{4}$	$\frac{1}{4}$	$\frac{1}{4}$	$\frac{1}{4}$	$\frac{1}{4}$	$\frac{1}{4}$	$-\frac{3}{4}$	$\frac{1}{4}$
153	$1 + q + r$	$\sigma_q \sigma_r \sigma_s$	0	0	0	0	0	0	-1	0
154	$p + pq + r$	$-\sigma_p \sigma_r \sigma_s J_{p,q}$	0	0	0	$\frac{1}{2}$	0	$\frac{1}{2}$	$-\frac{1}{2}$	$\frac{1}{2}$
155	$1 + q + pr + qr + pqr$	$\sigma_q \sigma_s J_{p,r} J_{q,r} K_{p,q,r}$	$-\frac{1}{4}$	$-\frac{1}{4}$	$-\frac{1}{4}$	$\frac{1}{4}$	$-\frac{1}{4}$	$-\frac{1}{4}$	$-\frac{3}{4}$	$\frac{1}{4}$
156	$p + q + pr$	$-\sigma_p \sigma_q \sigma_s J_{p,r}$	0	0	$\frac{1}{2}$	0	$\frac{1}{2}$	0	$-\frac{1}{2}$	$\frac{1}{2}$
157	$1 + pq + r + qr + pqr$	$\sigma_r \sigma_s J_{p,q} J_{q,r} K_{p,q,r}$	$-\frac{1}{4}$	$-\frac{1}{4}$	$\frac{1}{4}$	$-\frac{1}{4}$	$-\frac{1}{4}$	$-\frac{1}{4}$	$-\frac{3}{4}$	$\frac{1}{4}$
158	$p + q + r + qr + pqr$	$-\sigma_p \sigma_q \sigma_r \sigma_s J_{q,r} K_{p,q,r}$	$-\frac{1}{4}$	$-\frac{1}{4}$	$\frac{1}{4}$	$\frac{1}{4}$	$\frac{1}{4}$	$\frac{1}{4}$	$-\frac{1}{4}$	$\frac{3}{4}$
159	$1 + pq + pr$	$\sigma_s J_{p,q} J_{p,r}$	$-\frac{1}{2}$	$-\frac{1}{2}$	0	0	0	0	$-\frac{1}{2}$	$\frac{1}{2}$

TABLE VI: 2D classical spin models from 1D CA rules 120 to 159.

#### Appendix D: Numerics for OBC

Here we present similar numerical results for the quantum spin models in the case of open boundary conditions. Results are shown in Fig. 12 for  $H_{150}$ , in Fig. 13 for  $H_{\text{SPyM}}$ , and in Fig. 17 for the quantum Baxter-Wu model.

The presence of a quantum phase transition for  $H_{150}$  for OBC is obscured, as seen from Fig. 12 than in the PBC case. The existence of a subextensively increasing number of classical ground states, which correspond to low-lying states for the quantum model, affects the accuracy of the MPS simulations. For stripe geometries there is no indication of a discontinuity.

This situation resembles the one encountered for OBC for the TPM in Ref. [3]. The reasoning behind the difference between PBC and OBC is similar for all these models, as seen for  $H_{30}$  in Fig. 14, for  $H_{54}$  in Fig. 15 and for  $H_{201}$  in Fig. 16. For the 3D quantum SPyM with OBC, see Fig. 13, results are even less accurate due to the intrinsic limitations of our MPS simulations in 3D and the very restricted system sizes which are accessible.

For the quantum Baxter-Wu model with OBC, Fig. 17, we observe a different behaviour from that of the models above. The major discrepancy with PBC is that the transition has not converged to the value  $h = 2.4$  yet. Apart from this issue, nu-

CA rule no.	Update rule	$\mathcal{E}_{p,q,r,s}^{(\mu)}$	$\alpha_0$	$\alpha_{240}$	$\alpha_{204}$	$\alpha_{170}$	$\alpha_{60}$	$\alpha_{90}$	$\alpha_{102}$	$\alpha_{150}$
160	$pr$	$-\sigma_s J_{p,r}$	$\frac{1}{2}$	$\frac{1}{2}$	0	$\frac{1}{2}$	0	$-\frac{1}{2}$	0	0
161	$1+p+q+pq+r+qr+pqr$	$\sigma_p \sigma_q \sigma_r \sigma_s J_{p,q} J_{q,r} K_{p,q,r}$	$\frac{1}{4}$	$\frac{1}{4}$	$-\frac{1}{4}$	$\frac{1}{4}$	$-\frac{1}{4}$	$-\frac{3}{4}$	$-\frac{1}{4}$	$-\frac{1}{4}$
162	$r+qr+pqr$	$-\sigma_r \sigma_s J_{q,r} K_{p,q,r}$	$\frac{1}{4}$	$\frac{1}{4}$	$-\frac{1}{4}$	$\frac{1}{4}$	$-\frac{1}{4}$	$-\frac{1}{4}$	$\frac{1}{4}$	$\frac{1}{4}$
163	$1+p+q+pq+pr$	$\sigma_p \sigma_q \sigma_s J_{p,q} J_{p,r}$	0	0	$-\frac{1}{2}$	$\frac{1}{2}$	$-\frac{1}{2}$	$-\frac{1}{2}$	0	0
164	$q+pq+pr+qr+pqr$	$-\sigma_q \sigma_s J_{p,q} J_{p,r} J_{q,r} K_{p,q,r}$	$\frac{1}{4}$	$\frac{1}{4}$	$\frac{1}{4}$	$\frac{1}{4}$	$\frac{1}{4}$	$-\frac{3}{4}$	$\frac{1}{4}$	$\frac{1}{4}$
165	$1+p+r$	$\sigma_p \sigma_r \sigma_s$	0	0	0	0	0	-1	0	0
166	$q+pq+r$	$-\sigma_q \sigma_r \sigma_s J_{p,q}$	0	0	0	$\frac{1}{2}$	0	$-\frac{1}{2}$	$\frac{1}{2}$	$\frac{1}{2}$
167	$1+p+pr+qr+pqr$	$\sigma_p \sigma_s J_{p,r} J_{q,r} K_{p,q,r}$	$-\frac{1}{4}$	$-\frac{1}{4}$	$-\frac{1}{4}$	$\frac{1}{4}$	$-\frac{1}{4}$	$-\frac{3}{4}$	$\frac{1}{4}$	$\frac{1}{4}$
168	$pr+qr+pqr$	$-\sigma_s J_{p,r} J_{q,r} K_{p,q,r}$	$\frac{1}{4}$	$\frac{1}{4}$	$\frac{1}{4}$	$\frac{1}{4}$	$\frac{1}{4}$	$-\frac{1}{4}$	$-\frac{1}{4}$	$-\frac{1}{4}$
169	$1+p+q+pq+r$	$\sigma_p \sigma_q \sigma_r \sigma_s J_{p,q}$	0	0	0	$\frac{1}{2}$	0	$-\frac{1}{2}$	$-\frac{1}{2}$	$-\frac{1}{2}$
170	$r$	$-\sigma_r \sigma_s$	0	0	0	1	0	0	0	0
171	$1+p+q+pq+pr+qr+pqr$	$\sigma_p \sigma_q \sigma_s J_{p,q} J_{p,r} J_{q,r} K_{p,q,r}$	$-\frac{1}{4}$	$-\frac{1}{4}$	$-\frac{1}{4}$	$\frac{3}{4}$	$-\frac{1}{4}$	$-\frac{1}{4}$	$-\frac{1}{4}$	$-\frac{1}{4}$
172	$q+pq+pr$	$-\sigma_q \sigma_s J_{p,q} J_{p,r}$	0	0	$\frac{1}{2}$	$\frac{1}{2}$	$\frac{1}{2}$	$-\frac{1}{2}$	0	0
173	$1+p+r+qr+pqr$	$\sigma_p \sigma_r \sigma_s J_{q,r} K_{p,q,r}$	$-\frac{1}{4}$	$-\frac{1}{4}$	$\frac{1}{4}$	$\frac{1}{4}$	$\frac{1}{4}$	$-\frac{1}{4}$	$-\frac{1}{4}$	$-\frac{1}{4}$
174	$q+pq+r+qr+pqr$	$-\sigma_q \sigma_r \sigma_s J_{p,q} J_{q,r} K_{p,q,r}$	$-\frac{1}{4}$	$-\frac{1}{4}$	$\frac{1}{4}$	$\frac{1}{4}$	$\frac{1}{4}$	$-\frac{1}{4}$	$\frac{1}{4}$	$\frac{1}{4}$
175	$1+p+pr$	$\sigma_p \sigma_s J_{p,r}$	$-\frac{1}{2}$	$-\frac{1}{2}$	0	$\frac{1}{2}$	0	$-\frac{1}{2}$	0	0
176	$p+pq+pqr$	$-\sigma_p \sigma_s J_{p,q} K_{p,q,r}$	$\frac{1}{4}$	$\frac{3}{4}$	$-\frac{1}{4}$	$\frac{1}{4}$	$\frac{1}{4}$	$-\frac{1}{4}$	$-\frac{1}{4}$	$\frac{1}{4}$
177	$1+q+r+pr+qr$	$\sigma_q \sigma_r \sigma_s J_{p,r} J_{q,r}$	0	$\frac{1}{2}$	$-\frac{1}{2}$	0	0	$-\frac{1}{2}$	$-\frac{1}{2}$	0
178	$p+pq+r+pr+qr$	$-\sigma_p \sigma_r \sigma_s J_{p,q} J_{p,r} J_{q,r}$	0	$\frac{1}{2}$	$-\frac{1}{2}$	$\frac{1}{2}$	0	0	0	$\frac{1}{2}$
179	$1+q+pqr$	$\sigma_q \sigma_s K_{p,q,r}$	$-\frac{1}{4}$	$\frac{1}{4}$	$-\frac{3}{4}$	$\frac{1}{4}$	$-\frac{1}{4}$	$-\frac{1}{4}$	$-\frac{1}{4}$	$\frac{1}{4}$
180	$p+q+qr$	$-\sigma_p \sigma_q \sigma_s J_{q,r}$	0	$\frac{1}{2}$	0	0	$\frac{1}{2}$	$-\frac{1}{2}$	0	$\frac{1}{2}$
181	$1+pq+r+pr+pqr$	$\sigma_r \sigma_s J_{p,q} J_{p,r} K_{p,q,r}$	$-\frac{1}{4}$	$\frac{1}{4}$	$-\frac{1}{4}$	$-\frac{1}{4}$	$\frac{1}{4}$	$-\frac{3}{4}$	$-\frac{1}{4}$	$\frac{1}{4}$
182	$p+q+r+pr+pqr$	$-\sigma_p \sigma_q \sigma_r \sigma_s J_{p,r} K_{p,q,r}$	$-\frac{1}{4}$	$\frac{1}{4}$	$-\frac{1}{4}$	$\frac{1}{4}$	$\frac{1}{4}$	$-\frac{1}{4}$	$\frac{1}{4}$	$\frac{3}{4}$
183	$1+pq+qr$	$\sigma_s J_{p,q} J_{q,r}$	$-\frac{1}{2}$	0	$-\frac{1}{2}$	0	0	$-\frac{1}{2}$	0	$\frac{1}{2}$
184	$p+pq+qr$	$-\sigma_p \sigma_s J_{p,q} J_{q,r}$	0	$\frac{1}{2}$	0	$\frac{1}{2}$	$\frac{1}{2}$	0	$-\frac{1}{2}$	0
185	$1+q+r+pr+pqr$	$\sigma_q \sigma_r \sigma_s J_{p,r} K_{p,q,r}$	$-\frac{1}{4}$	$\frac{1}{4}$	$-\frac{1}{4}$	$\frac{1}{4}$	$\frac{1}{4}$	$-\frac{1}{4}$	$-\frac{3}{4}$	$-\frac{1}{4}$
186	$p+pq+r+pr+pqr$	$-\sigma_p \sigma_r \sigma_s J_{p,q} J_{p,r} K_{p,q,r}$	$-\frac{1}{4}$	$\frac{1}{4}$	$-\frac{1}{4}$	$\frac{1}{4}$	$\frac{1}{4}$	$-\frac{1}{4}$	$-\frac{1}{4}$	$\frac{1}{4}$
187	$1+q+qr$	$\sigma_q \sigma_s J_{q,r}$	$-\frac{1}{2}$	0	$-\frac{1}{2}$	$\frac{1}{2}$	0	0	$-\frac{1}{2}$	0
188	$p+q+pqr$	$-\sigma_p \sigma_q \sigma_s K_{p,q,r}$	$-\frac{1}{4}$	$\frac{1}{4}$	$\frac{1}{4}$	$\frac{1}{4}$	$\frac{3}{4}$	$-\frac{1}{4}$	$-\frac{1}{4}$	$\frac{1}{4}$
189	$1+pq+r+pr+qr$	$\sigma_r \sigma_s J_{p,q} J_{p,r} J_{q,r}$	$-\frac{1}{2}$	0	0	0	$\frac{1}{2}$	$-\frac{1}{2}$	$-\frac{1}{2}$	0
190	$p+q+r+pr+qr$	$-\sigma_p \sigma_q \sigma_r \sigma_s J_{p,r} J_{q,r}$	$-\frac{1}{2}$	0	0	$\frac{1}{2}$	$\frac{1}{2}$	0	0	$\frac{1}{2}$
191	$1+pq+pqr$	$\sigma_s J_{p,q} K_{p,q,r}$	$-\frac{3}{4}$	$-\frac{1}{4}$	$-\frac{1}{4}$	$\frac{1}{4}$	$\frac{1}{4}$	$-\frac{1}{4}$	$-\frac{1}{4}$	$\frac{1}{4}$
192	$pq$	$-\sigma_s J_{p,q}$	$\frac{1}{2}$	$\frac{1}{2}$	$\frac{1}{2}$	0	$-\frac{1}{2}$	0	0	0
193	$1+p+q+r+pr+qr+pqr$	$\sigma_p \sigma_q \sigma_r \sigma_s J_{p,r} J_{q,r} K_{p,q,r}$	$\frac{1}{4}$	$\frac{1}{4}$	$\frac{1}{4}$	$-\frac{1}{4}$	$-\frac{3}{4}$	$-\frac{1}{4}$	$-\frac{1}{4}$	$-\frac{1}{4}$
194	$pq+r+pr+qr+pqr$	$-\sigma_r \sigma_s J_{p,q} J_{p,r} J_{q,r} K_{p,q,r}$	$\frac{1}{4}$	$\frac{1}{4}$	$\frac{1}{4}$	$\frac{1}{4}$	$-\frac{1}{4}$	$\frac{1}{4}$	$\frac{1}{4}$	$\frac{1}{4}$
195	$1+p+q$	$\sigma_p \sigma_q \sigma_s$	0	0	0	0	-1	0	0	0
196	$q+qr+pqr$	$-\sigma_q \sigma_s J_{q,r} K_{p,q,r}$	$\frac{1}{4}$	$\frac{1}{4}$	$\frac{3}{4}$	$-\frac{1}{4}$	$-\frac{1}{4}$	$-\frac{1}{4}$	$\frac{1}{4}$	$\frac{1}{4}$
197	$1+p+pq+r+pr$	$\sigma_p \sigma_r \sigma_s J_{p,q} J_{p,r}$	0	0	$\frac{1}{2}$	$-\frac{1}{2}$	$-\frac{1}{2}$	$-\frac{1}{2}$	0	0
198	$q+r+pr$	$-\sigma_q \sigma_r \sigma_s J_{p,r}$	0	0	$\frac{1}{2}$	0	$-\frac{1}{2}$	0	$\frac{1}{2}$	$\frac{1}{2}$
199	$1+p+pq+qr+pqr$	$\sigma_p \sigma_s J_{p,q} J_{q,r} K_{p,q,r}$	$-\frac{1}{4}$	$-\frac{1}{4}$	$\frac{1}{4}$	$-\frac{1}{4}$	$-\frac{3}{4}$	$-\frac{1}{4}$	$\frac{1}{4}$	$\frac{1}{4}$

TABLE VII: 2D classical spin models from 1D CA rules 160 to 199.

merics seem to suggest that the phase transition for the quantum Baxter-Wu model with OBC is also first order, despite the convergence issues.

#### Appendix E: Low-lying energy spectra

Figure 18 shows the low-lying spectrum for two system sizes tractable via ED for  $H_{150}$ . In panel (b) we show the case of size  $4 \times 4$  for PBC: here we show the 16 lowest energy configurations given by the two fixed points (the all up and all down states) and 12 period 2 cycles of the CA, see Ta-

ble I; the avoided crossing at  $J = 1.0$  is the finite size signature of the eventual first order transition, while the splitting away from the ground state of levels 2 to 16 for  $h > 1$  is a signature of SSB of the symmetries. In panel (c) we show the same for a system size of  $3 \times 6$  where there are no limit cycles and the only classical minima are the all up and all down states; here it is enough to show the ground state and the first 2 excited states. Similarly to the PBC case, the energy spectrum from ED for the lowest energy states is presented for OBC in Fig. 18a. Similar behaviour to the PBC is observed. However, the state space involved in the SSB involves many more states ( $2^{2L+M-2}$  specifically for  $H_{150}$ ) and results in the avoided level

CA rule no.	Update rule	$\mathcal{E}_{p,q,r,s}^{(\mu)}$	$\alpha_0$	$\alpha_{240}$	$\alpha_{204}$	$\alpha_{170}$	$\alpha_{60}$	$\alpha_{90}$	$\alpha_{102}$	$\alpha_{150}$
200	$pq + qr + pqr$	$-\sigma_s J_{p,q} J_{q,r} K_{p,q,r}$	$\frac{1}{4}$	$\frac{1}{4}$	$\frac{3}{4}$	$\frac{1}{4}$	$-\frac{1}{4}$	$\frac{1}{4}$	$-\frac{1}{4}$	$-\frac{1}{4}$
201	$1 + p + q + r + pr$	$\sigma_p \sigma_q \sigma_r \sigma_s J_{p,r}$	0	0	$\frac{1}{2}$	0	$-\frac{1}{2}$	0	$-\frac{1}{2}$	$-\frac{1}{2}$
202	$pq + r + pr$	$-\sigma_r \sigma_s J_{p,q} J_{p,r}$	0	0	$\frac{1}{2}$	$\frac{1}{2}$	$-\frac{1}{2}$	$\frac{1}{2}$	0	0
203	$1 + p + q + qr + pqr$	$\sigma_p \sigma_q \sigma_s J_{q,r} K_{p,q,r}$	$-\frac{1}{4}$	$-\frac{1}{4}$	$\frac{1}{4}$	$\frac{1}{4}$	$-\frac{3}{4}$	$\frac{1}{4}$	$-\frac{1}{4}$	$-\frac{1}{4}$
204	$q$	$-\sigma_q \sigma_s$	0	0	1	0	0	0	0	0
205	$1 + p + pq + r + pr + qr + pqr$	$\sigma_p \sigma_r \sigma_s J_{p,q} J_{p,r} J_{q,r} K_{p,q,r}$	$-\frac{1}{4}$	$-\frac{1}{4}$	$\frac{3}{4}$	$-\frac{1}{4}$	$-\frac{1}{4}$	$-\frac{1}{4}$	$-\frac{1}{4}$	$-\frac{1}{4}$
206	$q + r + pr + qr + pqr$	$-\sigma_q \sigma_r \sigma_s J_{p,r} J_{q,r} K_{p,q,r}$	$-\frac{1}{4}$	$-\frac{1}{4}$	$\frac{3}{4}$	$\frac{1}{4}$	$-\frac{1}{4}$	$\frac{1}{4}$	$\frac{1}{4}$	$\frac{1}{4}$
207	$1 + p + pq$	$\sigma_p \sigma_s J_{p,q}$	$-\frac{1}{2}$	$-\frac{1}{2}$	$\frac{1}{2}$	0	$-\frac{1}{2}$	0	0	0
208	$p + pr + pqr$	$-\sigma_p \sigma_s J_{p,r} K_{p,q,r}$	$\frac{1}{4}$	$\frac{1}{4}$	$\frac{1}{4}$	$-\frac{1}{4}$	$-\frac{1}{4}$	$\frac{1}{4}$	$-\frac{1}{4}$	$\frac{1}{4}$
209	$1 + q + pq + r + qr$	$\sigma_q \sigma_r \sigma_s J_{p,q} J_{q,r}$	0	$\frac{1}{2}$	0	$-\frac{1}{2}$	$-\frac{1}{2}$	0	$-\frac{1}{2}$	0
210	$p + r + qr$	$-\sigma_p \sigma_r \sigma_s J_{q,r}$	0	$\frac{1}{2}$	0	0	$-\frac{1}{2}$	$\frac{1}{2}$	0	$\frac{1}{2}$
211	$1 + q + pq + pr + pqr$	$\sigma_q \sigma_s J_{p,q} J_{p,r} K_{p,q,r}$	$-\frac{1}{4}$	$\frac{1}{4}$	$-\frac{1}{4}$	$-\frac{1}{4}$	$-\frac{3}{4}$	$\frac{1}{4}$	$-\frac{1}{4}$	$\frac{1}{4}$
212	$p + q + pq + pr + qr$	$-\sigma_p \sigma_q \sigma_s J_{p,q} J_{p,r} J_{q,r}$	0	$\frac{1}{2}$	$\frac{1}{2}$	$-\frac{1}{2}$	0	0	0	$\frac{1}{2}$
213	$1 + r + pqr$	$\sigma_r \sigma_s K_{p,q,r}$	$-\frac{1}{4}$	$\frac{1}{4}$	$\frac{1}{4}$	$-\frac{1}{4}$	$-\frac{1}{4}$	$-\frac{1}{4}$	$-\frac{1}{4}$	$\frac{1}{4}$
214	$p + q + pq + r + pqr$	$-\sigma_p \sigma_q \sigma_r \sigma_s J_{p,q} K_{p,q,r}$	$-\frac{1}{4}$	$\frac{1}{4}$	$\frac{1}{4}$	$-\frac{1}{4}$	$-\frac{1}{4}$	$\frac{1}{4}$	$\frac{1}{4}$	$\frac{3}{4}$
215	$1 + pr + qr$	$\sigma_s J_{p,r} J_{q,r}$	$-\frac{1}{2}$	0	0	$-\frac{1}{2}$	0	0	0	$\frac{1}{2}$
216	$p + pr + qr$	$-\sigma_p \sigma_s J_{p,r} J_{q,r}$	0	$\frac{1}{2}$	$\frac{1}{2}$	0	0	$\frac{1}{2}$	$-\frac{1}{2}$	0
217	$1 + q + pq + r + pqr$	$\sigma_q \sigma_r \sigma_s J_{p,q} K_{p,q,r}$	$-\frac{1}{4}$	$\frac{1}{4}$	$\frac{1}{4}$	$-\frac{1}{4}$	$-\frac{1}{4}$	$-\frac{1}{4}$	$-\frac{1}{4}$	$-\frac{1}{4}$
218	$p + r + pqr$	$-\sigma_p \sigma_r \sigma_s K_{p,q,r}$	$-\frac{1}{4}$	$\frac{1}{4}$	$\frac{1}{4}$	$\frac{1}{4}$	$-\frac{1}{4}$	$\frac{3}{4}$	$-\frac{1}{4}$	$\frac{1}{4}$
219	$1 + q + pq + pr + qr$	$\sigma_q \sigma_s J_{p,q} J_{p,r} J_{q,r}$	$-\frac{1}{2}$	0	0	0	$-\frac{1}{2}$	$\frac{1}{2}$	$-\frac{1}{2}$	0
220	$p + q + pq + pr + pqr$	$-\sigma_p \sigma_q \sigma_s J_{p,q} J_{p,r} K_{p,q,r}$	$-\frac{1}{4}$	$\frac{1}{4}$	$\frac{3}{4}$	$-\frac{1}{4}$	$\frac{1}{4}$	$\frac{1}{4}$	$-\frac{1}{4}$	$\frac{1}{4}$
221	$1 + r + qr$	$\sigma_r \sigma_s J_{q,r}$	$-\frac{1}{2}$	0	$\frac{1}{2}$	$-\frac{1}{2}$	0	0	$-\frac{1}{2}$	0
222	$p + q + pq + r + qr$	$-\sigma_p \sigma_q \sigma_r \sigma_s J_{p,q} J_{q,r}$	$-\frac{1}{2}$	0	$\frac{1}{2}$	0	0	$\frac{1}{2}$	0	$\frac{1}{2}$
223	$1 + pr + pqr$	$\sigma_s J_{p,r} K_{p,q,r}$	$-\frac{3}{4}$	$-\frac{1}{4}$	$\frac{1}{4}$	$-\frac{1}{4}$	$-\frac{1}{4}$	$\frac{1}{4}$	$-\frac{1}{4}$	$\frac{1}{4}$
224	$pq + pr + pqr$	$-\sigma_s J_{p,q} J_{p,r} K_{p,q,r}$	$\frac{1}{4}$	$\frac{3}{4}$	$\frac{1}{4}$	$\frac{1}{4}$	$-\frac{1}{4}$	$-\frac{1}{4}$	$\frac{1}{4}$	$-\frac{1}{4}$
225	$1 + p + q + r + qr$	$\sigma_p \sigma_q \sigma_r \sigma_s J_{q,r}$	0	$\frac{1}{2}$	0	0	$-\frac{1}{2}$	$-\frac{1}{2}$	0	$-\frac{1}{2}$
226	$pq + r + qr$	$-\sigma_r \sigma_s J_{p,q} J_{q,r}$	0	$\frac{1}{2}$	0	$\frac{1}{2}$	$-\frac{1}{2}$	0	$\frac{1}{2}$	0
227	$1 + p + q + pr + pqr$	$\sigma_p \sigma_q \sigma_s J_{p,r} K_{p,q,r}$	$-\frac{1}{4}$	$\frac{1}{4}$	$-\frac{1}{4}$	$\frac{1}{4}$	$-\frac{3}{4}$	$-\frac{1}{4}$	$\frac{1}{4}$	$-\frac{1}{4}$
228	$q + pr + qr$	$-\sigma_q \sigma_s J_{p,r} J_{q,r}$	0	$\frac{1}{2}$	$\frac{1}{2}$	0	0	$-\frac{1}{2}$	$\frac{1}{2}$	0
229	$1 + p + pq + r + pqr$	$\sigma_p \sigma_r \sigma_s J_{p,q} K_{p,q,r}$	$-\frac{1}{4}$	$\frac{1}{4}$	$\frac{1}{4}$	$-\frac{1}{4}$	$-\frac{1}{4}$	$-\frac{3}{4}$	$\frac{1}{4}$	$-\frac{1}{4}$
230	$q + r + pqr$	$-\sigma_q \sigma_r \sigma_s K_{p,q,r}$	$-\frac{1}{4}$	$\frac{1}{4}$	$\frac{1}{4}$	$\frac{1}{4}$	$-\frac{1}{4}$	$-\frac{1}{4}$	$\frac{3}{4}$	$\frac{1}{4}$
231	$1 + p + pq + pr + qr$	$\sigma_p \sigma_s J_{p,q} J_{p,r} J_{q,r}$	$-\frac{1}{2}$	0	0	0	$-\frac{1}{2}$	$-\frac{1}{2}$	$\frac{1}{2}$	0
232	$pq + pr + qr$	$-\sigma_s J_{p,q} J_{p,r} J_{q,r}$	0	$\frac{1}{2}$	$\frac{1}{2}$	$\frac{1}{2}$	0	0	0	$-\frac{1}{2}$
233	$1 + p + q + r + pqr$	$\sigma_p \sigma_q \sigma_r \sigma_s K_{p,q,r}$	$-\frac{1}{4}$	$\frac{1}{4}$	$\frac{1}{4}$	$\frac{1}{4}$	$-\frac{1}{4}$	$-\frac{1}{4}$	$-\frac{1}{4}$	$-\frac{1}{4}$
234	$pq + r + pqr$	$-\sigma_r \sigma_s J_{p,q} K_{p,q,r}$	$-\frac{1}{4}$	$\frac{1}{4}$	$\frac{1}{4}$	$\frac{1}{4}$	$-\frac{1}{4}$	$\frac{1}{4}$	$\frac{1}{4}$	$-\frac{1}{4}$
235	$1 + p + q + pr + qr$	$\sigma_p \sigma_q \sigma_s J_{p,r} J_{q,r}$	$-\frac{1}{2}$	0	0	$\frac{1}{2}$	$-\frac{1}{2}$	0	0	$-\frac{1}{2}$
236	$q + pr + pqr$	$-\sigma_q \sigma_s J_{p,r} K_{p,q,r}$	$-\frac{1}{4}$	$\frac{1}{4}$	$\frac{3}{4}$	$\frac{1}{4}$	$-\frac{1}{4}$	$-\frac{1}{4}$	$\frac{1}{4}$	$-\frac{1}{4}$
237	$1 + p + pq + r + qr$	$\sigma_p \sigma_r \sigma_s J_{p,q} J_{q,r}$	$-\frac{1}{2}$	0	$\frac{1}{2}$	0	0	$-\frac{1}{2}$	0	$-\frac{1}{2}$
238	$q + r + qr$	$-\sigma_q \sigma_r \sigma_s J_{q,r}$	$-\frac{1}{2}$	0	$\frac{1}{2}$	$\frac{1}{2}$	0	0	$\frac{1}{2}$	0
239	$1 + p + pq + pr + pqr$	$\sigma_p \sigma_s J_{p,q} J_{p,r} K_{p,q,r}$	$-\frac{3}{4}$	$-\frac{1}{4}$	$\frac{1}{4}$	$\frac{1}{4}$	$-\frac{1}{4}$	$-\frac{1}{4}$	$\frac{1}{4}$	$-\frac{1}{4}$

TABLE VIII: 2D classical spin models from 1D CA rules 200 to 239.

crossing which would signal the first order behaviour of the transition to be hidden.

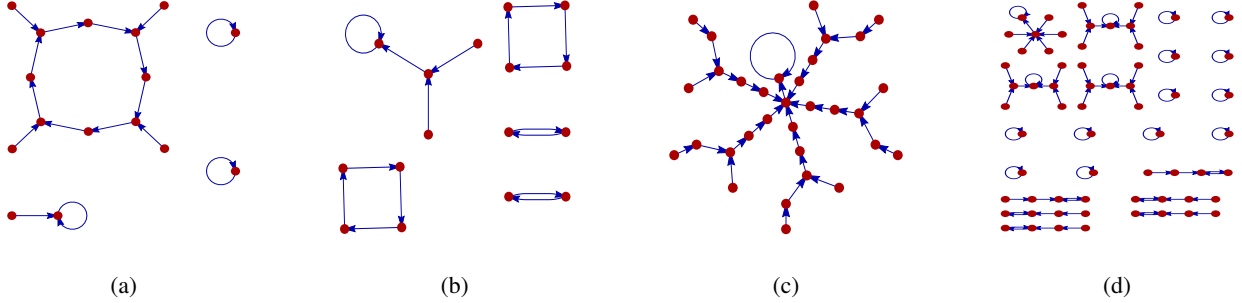
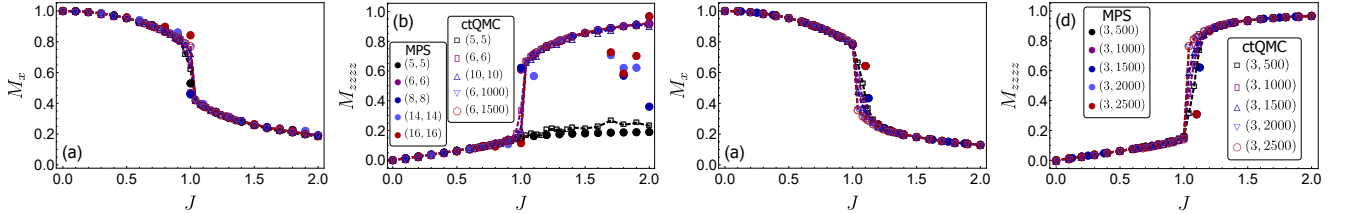
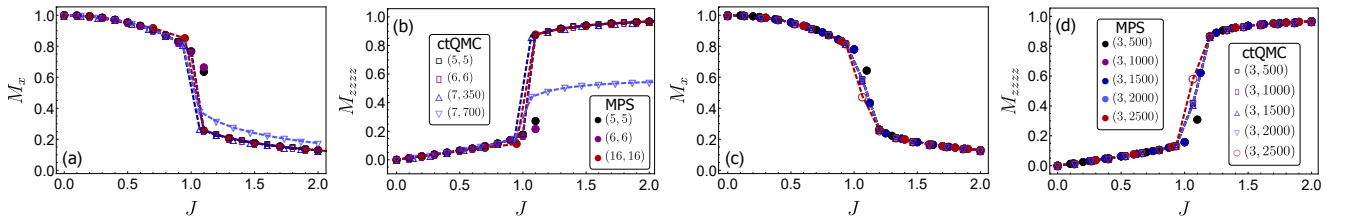
Similar arguments lead to the same conclusions for the energy spectrum for the quantum rule 30 from Fig. 19. The situation becomes progressively worse for the quantum rules 30, 54 and 201 in Figs. 19,20,21, respectively. The avoided gap crossing is easily observed for the  $3 \times 6$  system size for the quantum rule 54. However, no system size shows the avoided gap crossing for the quantum rule 201 for any of its low-lying states. It is important to note here that in Figs. 19,20,21 we

have omitted some energy levels which do not lead to any further conclusion. For example, for the quantum rule 30 and for a  $3 \times 6$  system size the third to the twelfth energy levels are omitted as they are just lying between the first excited state and the 13th excited state which is responsible for the avoided gap crossing without providing any further information to the given graphs. Similarly, there are cases where the energy level which is responsible for the avoided gap crossing involves a much higher excited mode and no clear indication of the gap closing for the given, small system sizes shown.



CA rule no.	Update rule	$\varepsilon_{p,q,r,s}^{(\mu)}$	$\alpha_0$	$\alpha_{240}$	$\alpha_{204}$	$\alpha_{170}$	$\alpha_{60}$	$\alpha_{90}$	$\alpha_{102}$	$\alpha_{150}$
240	$p$	$-\sigma_p \sigma_s$	0	1	0	0	0	0	0	0
241	$1 + q + pq + r + pr + qr + pqr$	$\sigma_q \sigma_r \sigma_s J_{p,q} J_{p,r} J_{q,r} K_{p,q,r}$	$-\frac{1}{4}$	$\frac{3}{4}$	$-\frac{1}{4}$	$-\frac{1}{4}$	$-\frac{1}{4}$	$-\frac{1}{4}$	$-\frac{1}{4}$	$-\frac{1}{4}$
242	$p + r + pr + qr + pqr$	$-\sigma_p \sigma_r \sigma_s J_{p,r} J_{q,r} K_{p,q,r}$	$-\frac{1}{4}$	$\frac{3}{4}$	$-\frac{1}{4}$	$\frac{1}{4}$	$-\frac{1}{4}$	$\frac{1}{4}$	$\frac{1}{4}$	$\frac{1}{4}$
243	$1 + q + pq$	$\sigma_q \sigma_s J_{p,q}$	$-\frac{1}{2}$	$\frac{1}{2}$	$-\frac{1}{2}$	0	$-\frac{1}{2}$	0	0	0
244	$p + q + pq + qr + pqr$	$-\sigma_p \sigma_q \sigma_s J_{p,q} J_{q,r} K_{p,q,r}$	$-\frac{1}{4}$	$\frac{3}{4}$	$\frac{1}{4}$	$-\frac{1}{4}$	$\frac{1}{4}$	$-\frac{1}{4}$	$\frac{1}{4}$	$\frac{1}{4}$
245	$1 + r + pr$	$\sigma_r \sigma_s J_{p,r}$	$-\frac{1}{2}$	$\frac{1}{2}$	0	$-\frac{1}{2}$	0	$-\frac{1}{2}$	0	0
246	$p + q + pq + r + pr$	$-\sigma_p \sigma_q \sigma_r \sigma_s J_{p,q} J_{p,r}$	$-\frac{1}{3}$	$\frac{2}{3}$	0	0	0	0	$\frac{1}{2}$	$\frac{1}{2}$
247	$1 + qr + pqr$	$\sigma_s J_{q,r} K_{p,q,r}$	$-\frac{3}{4}$	$\frac{1}{4}$	$-\frac{1}{4}$	$-\frac{1}{4}$	$-\frac{1}{4}$	$-\frac{1}{4}$	$\frac{1}{4}$	$\frac{1}{4}$
248	$p + qr + pqr$	$-\sigma_p \sigma_s J_{q,r} K_{p,q,r}$	$-\frac{1}{4}$	$\frac{3}{4}$	$\frac{1}{4}$	$\frac{1}{4}$	$\frac{1}{4}$	$-\frac{1}{4}$	$-\frac{1}{4}$	$-\frac{1}{4}$
249	$1 + q + pq + r + pr$	$\sigma_q \sigma_r \sigma_s J_{p,q} J_{p,r}$	$-\frac{1}{2}$	$\frac{1}{2}$	0	0	0	0	$-\frac{1}{2}$	$-\frac{1}{2}$
250	$p + r + pr$	$-\sigma_p \sigma_r \sigma_s J_{p,r}$	$-\frac{1}{2}$	$\frac{1}{2}$	0	$\frac{1}{2}$	0	$\frac{1}{2}$	0	0
251	$1 + q + pq + qr + pqr$	$\sigma_q \sigma_s J_{p,q} J_{q,r} K_{p,q,r}$	$-\frac{1}{4}$	$\frac{3}{4}$	$-\frac{1}{4}$	$\frac{1}{4}$	$-\frac{1}{4}$	$\frac{1}{4}$	$-\frac{1}{4}$	$-\frac{1}{4}$
252	$p + q + pq$	$-\sigma_p \sigma_q \sigma_s J_{p,q}$	$-\frac{1}{2}$	$\frac{1}{2}$	$\frac{1}{2}$	0	0	0	0	0
253	$1 + r + pr + qr + pqr$	$\sigma_r \sigma_s J_{p,r} J_{q,r} K_{p,q,r}$	$-\frac{3}{4}$	$\frac{1}{4}$	$\frac{1}{4}$	$-\frac{1}{4}$	$\frac{1}{4}$	$-\frac{1}{4}$	$-\frac{1}{4}$	$-\frac{1}{4}$
254	$p + q + pq + r + pr + qr + pqr$	$-\sigma_p \sigma_q \sigma_r \sigma_s J_{p,q} J_{p,r} J_{q,r} K_{p,q,r}$	$-\frac{1}{4}$	$\frac{3}{4}$	$\frac{1}{4}$	$\frac{1}{4}$	$\frac{1}{4}$	$\frac{1}{4}$	$\frac{1}{4}$	$\frac{1}{4}$
255	1	$\sigma_s$	-1	0	0	0	0	0	0	0

TABLE IX: 2D classical spin models from 1D CA rules 240 to 255.

FIG. 8: The attractor and fixed point structure of (a) rule 30 with  $L = 4$ , (b) rule 54 with  $L = 4$ , (c) rule 54 with  $L = 5$  and (d) rule 201 for  $L = 6$ .FIG. 9: **Quantum phase transition of  $H_{30}$  for PBC.** (a) Transverse magnetisation  $M_x$  as a function of  $J$ , for square system sizes  $L \times L$  from numerical MPS (filled symbols) and square and rectangular sizes from ctQMC simulations (empty symbols). (b) Four-spin interaction magnetisation similar to (a). (c,d) Same with (a, b) for thin stripe system sizes.FIG. 10: **Quantum phase transition of  $H_{54}$  for PBC, similar to Fig. 9.**

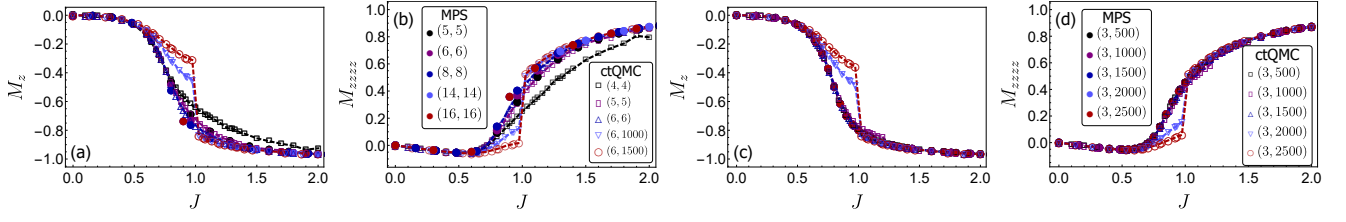


FIG. 11: Quantum phase transition of  $H_{201}$  for PBC, similar to Fig. 9.

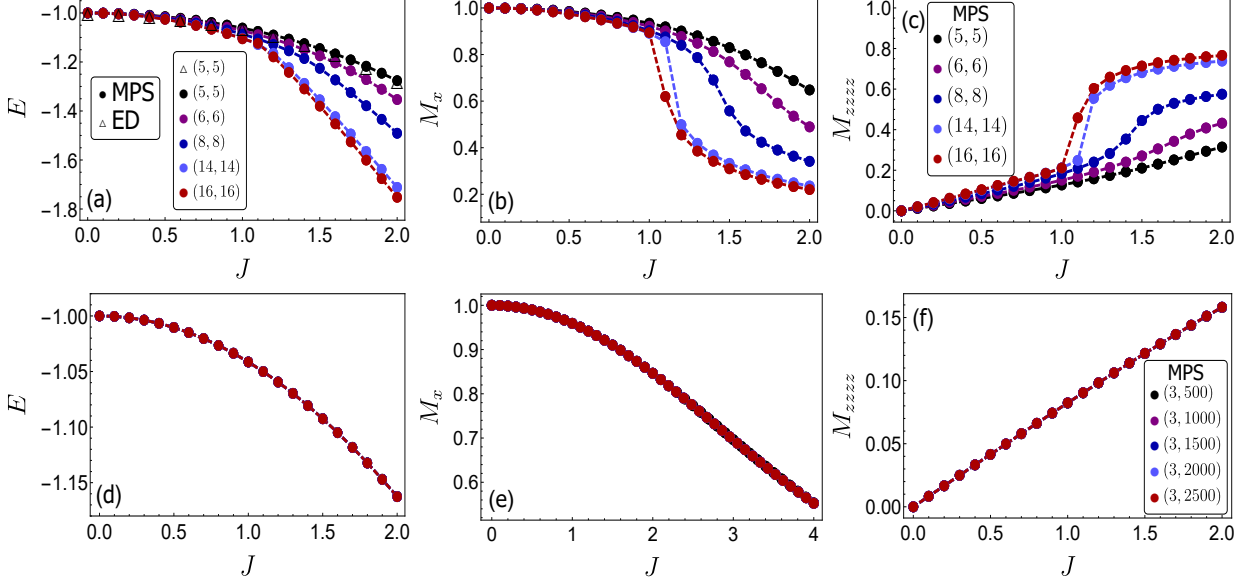


FIG. 12: Quantum phase transition of  $H_{150}$  for OBC. (a) The normalised by the system size ground state energy as a function of  $J$ . Empty symbols are from ED while filled symbols are from numerical MPS. (b) Transverse magnetisation as a function of  $J$ . (c) Average four-spin interaction as a function of  $J$ . (d-f) Similar to (a-c) but for the rectangular system sizes given in the inset of panel (f).

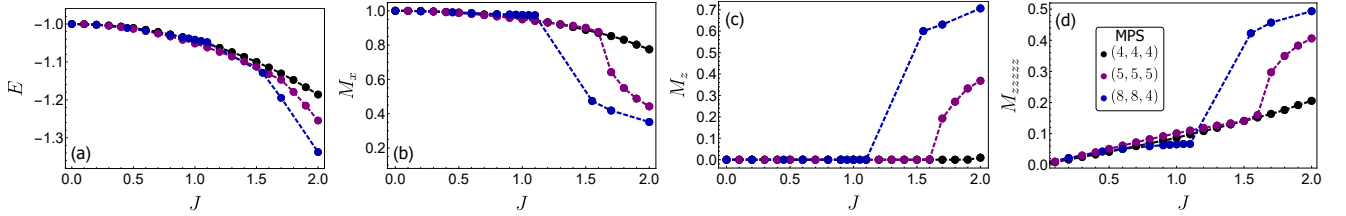


FIG. 13: Quantum phase transition of  $H_{SPyM}$  for OBC. (a) Ground state energy,  $E$ , per unit size as a function of  $J$ , for system sizes  $L \times L \times M$ . (b-d) The transverse and longitudinal magnetisations and the average five-spin interaction, respectively.

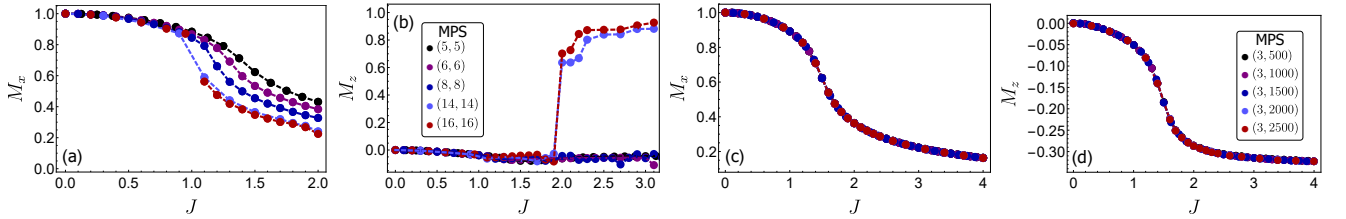


FIG. 14: Quantum phase transition of  $H_{30}$  for OBC. (a,b) Transverse magnetisation  $M_x$  and longitudinal magnetisation as a function of  $J$  for square system sizes. (c,d) Same for rectangular system sizes.

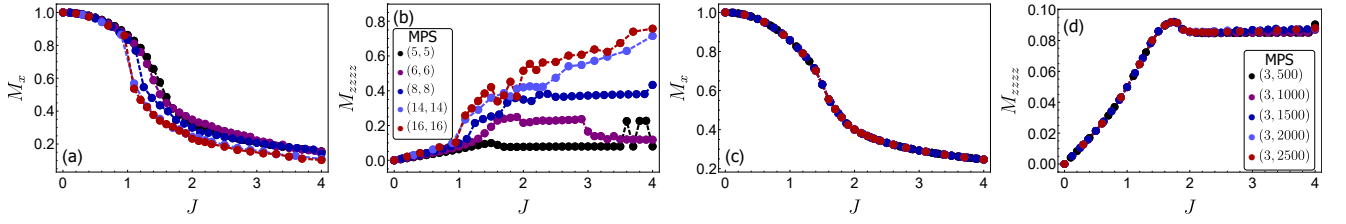


FIG. 15: **Quantum phase transition of  $H_{54}$  for OBC.** (a,b) Transverse magnetisation  $M_x$  and four-spin interaction as a function of  $J$  for square system sizes. (c,d) Same for rectangular system sizes.

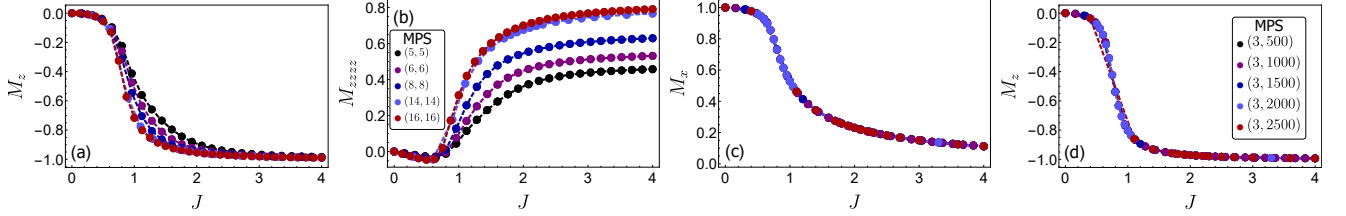


FIG. 16: **Quantum phase transition of  $H_{201}$  for OBC.** (a) Longitudinal magnetisation  $M_z$  and four-spin interaction as a function of  $J$  for square system sizes. (c,d) Same for rectangular system sizes for the transverse and longitudinal magnetisations.

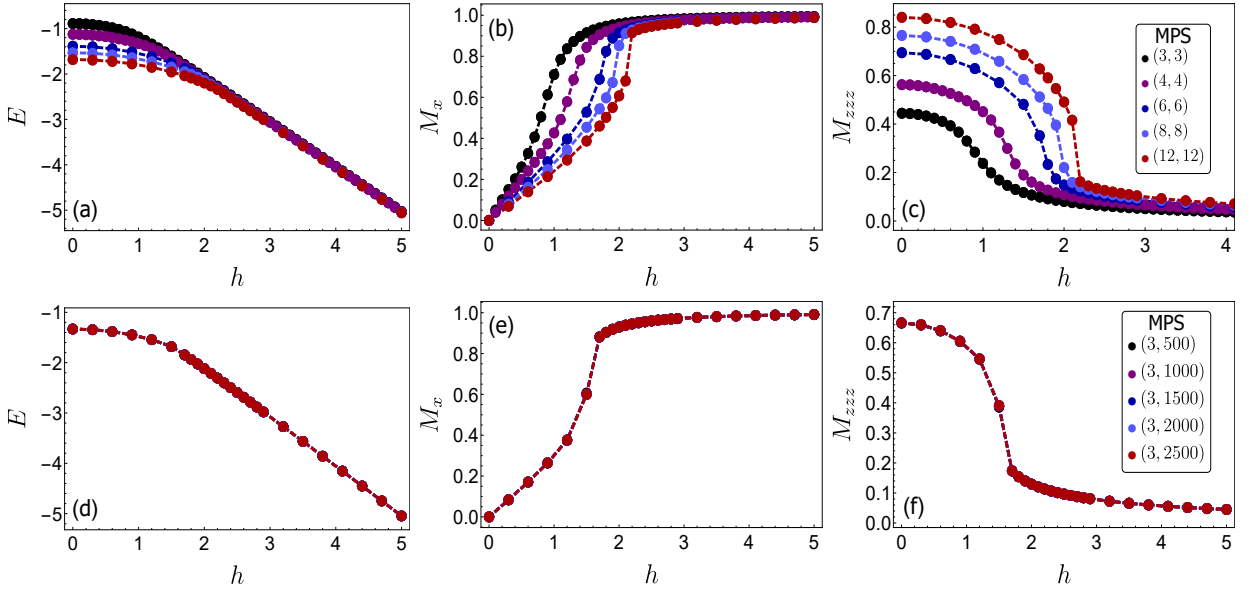


FIG. 17: **Quantum phase transition of the qBW model for OBC.** (a) The normalised by the system size ground state energy as a function of  $h$ . (b,c) Transverse magnetisation and three-spin correlator for the interaction of Rule 60 as a function of  $h$ . (d-f) Similar to (a-c) but for the rectangular system sizes given in the inset of panel (f).

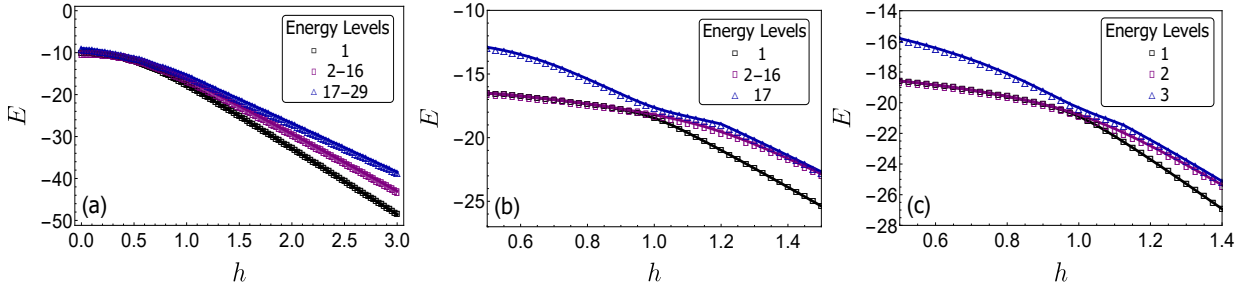


FIG. 18: **Low-lying spectrum of  $H_{150}$ .** (a) Ground state (level 1) and the first 28 excited states (levels 2-29) as a function of  $h$  for a system size  $4 \times 4$  for OBC. As seen from this panel, the avoided gap crossing is not formed by any of the low-lying states, but involves a higher excited state. (b) Ground state (level 1) and the first 16 excited states (levels 2-17) as a function of  $h$  for a system size  $4 \times 4$  for PBC. The avoided crossing is indicative of a first order transition in the ground state, while the splitting of excited levels that of SSB. (c) Same with (b) for the first 3 levels of a system size  $3 \times 6$  for PBC.

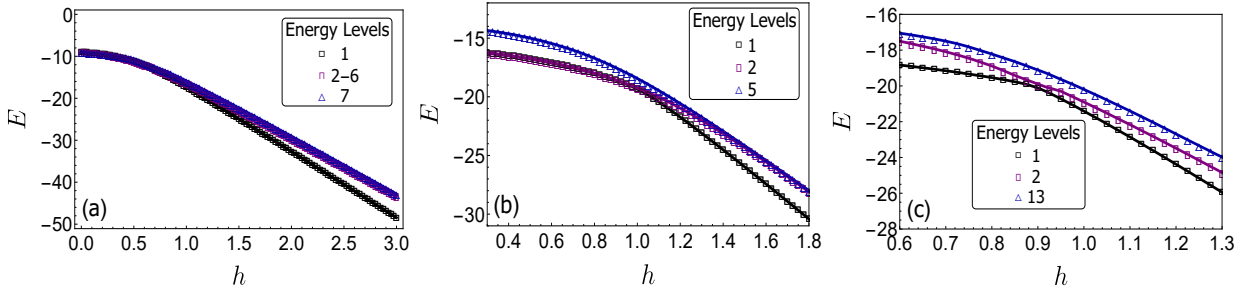


FIG. 19: **Low-lying spectrum of  $H_{30}$**  similar to Fig. 18 for a  $4 \times 4$  system size with OBC (a), a  $4 \times 4$  (b) and a  $3 \times 6$  (c) system size for PBC for their respective modes. The avoided gap crossing is evident in panels (b) and (c), similar to Fig. 18.

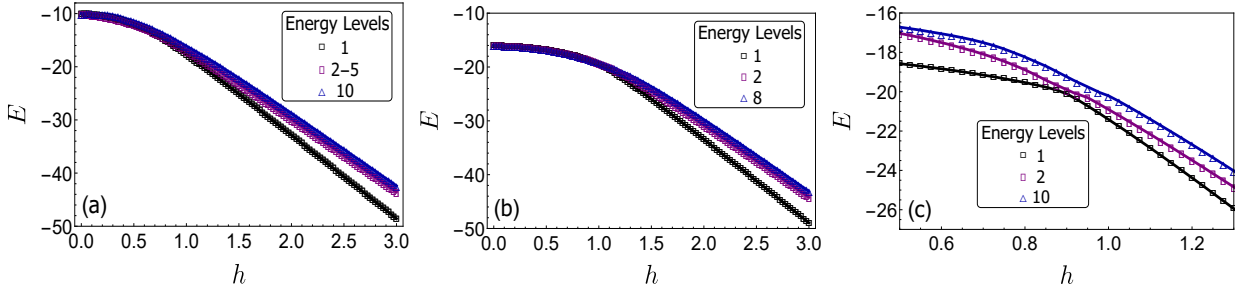


FIG. 20: **Low-lying spectrum of  $H_{54}$**  similar to Fig. 19. The avoided gap crossing is evident only in panel (c).

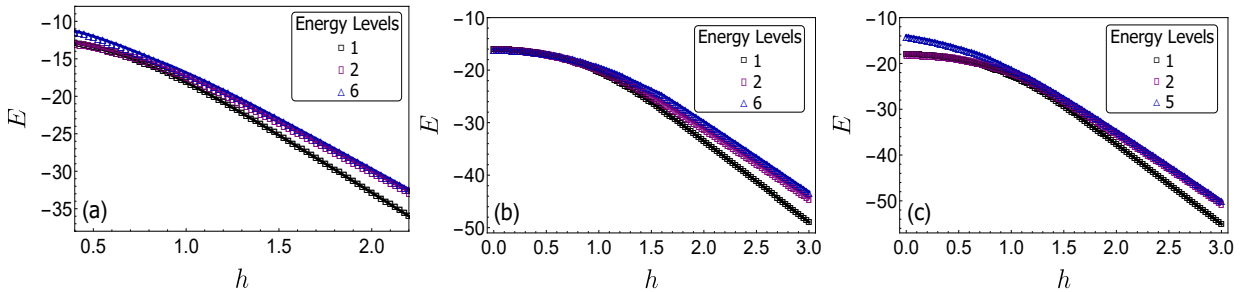


FIG. 21: **Low-lying spectrum of  $H_{201}$**  similar to Fig. 19. The avoided gap crossing is evident only in panel (c).

L	C
3	1
4	8, 1
5	5, 1
6	1
7	63, 4, 1
8	40, 8, 1
9	171, 72, 1
10	15, 5, 1
11	154, 17, 1
12	102, 8, 3, 1
13	832, 260, 247, 91, 1
14	1428, 133, 112, 84, 63, 14, 4, 1
15	1455, 30, 9, 7, 5, 1
16	6016, 4144, 40, 8, 1
17	10846, 1632, 867, 306, 136, 17, 1
18	2844, 186, 171, 72, 24, 1
19	3705, 247, 133, 38, 1
20	6150, 3420, 1715, 580, 68, 30, 15, 8, 5, 1
21	2793, 597, 409, 63, 44, 42, 4, 1
22	3553, 3256, 781, 154, 77, 66, 17, 1
23	38249, 4784, 138, 1
24	185040, 5448, 366, 312, 102, 40, 20, 8, 3, 1
25	588425, 2950, 74525, 3470, 275, 5, 1

TABLE X: Periods for rule 30.

L	C
3	1
4	4, 2, 1
5	1
6	4, 1
7	4, 1
8	8, 6, 4, 2, 1
9	27, 4, 1
10	30, 4, 1
11	99, 11, 4, 1
12	12, 10, 4, 2, 1
13	169, 4, 1
14	112, 4, 1
15	330, 4, 1
16	40, 16, 14, 8, 6, 4, 2, 1
17	289, 51, 4, 1
18	306, 90, 180, 4, 1
19	494, 437, 247, 57, 54, 27, 19, 4, 1
20	86, 60, 48, 32, 30, 24, 20, 18, 4, 2, 1
21	399, 147, 63, 14, 4, 1
22	484, 264, 242, 198, 121, 99, 32, 11, 4, 1
23	52371, 690, 575, 4, 1
24	312, 98, 56, 42, 32, 24, 22, 12, 10, 8, 6, 4, 2, 1
25	1800, 550, 115, 75, 4, 1
26	624, 546, 520, 338, 182, 169, 120, 78, 32, 26, 14, 4, 1
27	918, 837, 783, 459, 243, 81, 80, 27, 4, 1
28	224, 112, 110, 84, 64, 34, 32, 28, 26, 4, 2, 1
29	783, 725, 464, 203, 87, 80, 18, 4, 1
30	780, 750, 660, 630, 420, 330, 150, 90, 75, 32, 30, 4, 1
31	1240, 1178, 1023, 961, 651, 450, 341, 217, 93, 42, 4, 1
32	608, 544, 144, 122, 96, 72, 40, 36, 32, 30, 22, 16, 14, 8, 6, 4, 2, 1
33	1056, 1023, 957, 858, 429, 297, 143, 111, 99, 48, 11, 4, 1
34	952, 850, 816, 782, 578, 544, 289, 272, 119, 102, 51, 36, 34, 32, 4, 1
35	1540, 1470, 1225, 770, 735, 185, 105, 54, 35, 4, 1

TABLE XI: Periods for rule 54.